Measurement of normalized differential tt¯ cross sections in the dilepton channel from pp collisions at √s = 13 TeV

Published for SISSA by Springer

Received: *August 25, 2017*
Revised: *December 1, 2017*
Accepted: *March 27, 2018*
Published: *April 11, 2018*

Measurement of normalized differential $\mathrm{t\bar{t}}$ cross sections in the dilepton channel from pp collisions at $\sqrt{s} = 13\,\mathrm{TeV}$

The CMS collaboration

E-mail: cms-publication-committee-chair@cern.ch

Abstract: Normalized differential cross sections for top quark pair production are measured in the dilepton ($\mathrm{e^+e^-}$, $\mu^+\mu^-$, and $\mu^\mp\mathrm{e}^\pm$) decay channels in proton-proton collisions at a center-of-mass energy of 13 TeV. The measurements are performed with data corresponding to an integrated luminosity of 2.1 fb^{-1} using the CMS detector at the LHC. The cross sections are measured differentially as a function of the kinematic properties of the leptons, jets from bottom quark hadronization, top quarks, and top quark pairs at the particle and parton levels. The results are compared to several Monte Carlo generators that implement calculations up to next-to-leading order in perturbative quantum chromodynamics interfaced with parton showering, and also to fixed-order theoretical calculations of top quark pair production up to next-to-next-to-leading order.

Keywords: Hadron-Hadron scattering (experiments), Top physics, Heavy quark production, QCD

ArXiv ePrint: 1708.07638

https://doi.org/10.1007/JHEP04(2018)060

JHEP04(2018)060

Contents

JHEP04(2018)060

1 Introduction

The measurement of $t\bar{t}$ differential cross sections can provide a test of perturbative quantum chromodynamic (QCD) calculations and also improve the knowledge of parton distribution functions (PDFs) [1]. Previous measurements of differential cross sections for $t\bar{t}$ production have been performed in proton-proton (pp) collisions at the CERN LHC at center-of-mass energies of 7 [2, 3] and 8 TeV [4–12]. The dilepton (electron or muon) final state of the $t\bar{t}$ decay helps in the suppression of background events. This paper presents the first CMS measurement at $\sqrt{s} = 13$ TeV in the dilepton decay final state and includes the same-flavor lepton channels (e^+e^- and $\mu^+\mu^-$), using data corresponding to an integrated luminosity of 2.1 fb^{-1}. The statistical precision of the measurements is improved by the increased data sample from including the same-flavor lepton channels. The data were recorded by the CMS experiment at the LHC in 2015, and this measurement complements other recent

measurements that have been reported in a different decay channel [13] and by a different experiment [14, 15].

The $\mathrm{t\bar{t}}$ differential cross section measurements are performed at the particle and parton levels. Particle-level measurements use final-state kinematic observables that are experimentally measurable and theoretically well defined. Corrections are limited mainly to detector effects that can be determined experimentally. The particle-level measurements are designed to have minimal model dependencies. The visible differential cross section is defined for a phase space within the acceptance of the experiment. Large extrapolations into inaccessible phase-space regions are thus avoided in particle-level differential cross section measurements. In contrast, the parton-level measurement of the top quark pair production cross sections is performed in the full phase space. This facilitates comparisons to predictions in perturbative QCD.

The normalized $\mathrm{t\bar{t}}$ differential cross sections are measured as a function of the kinematic properties of the $\mathrm{t\bar{t}}$ system, the top quarks and the top quark decay products, which include the jets coming from the hadronization of bottom quarks and the leptons. The particle-level measurements are performed with respect to the transverse momentum of the leptons and of the jets. The cross sections as a function of the invariant mass and rapidity of the $\mathrm{t\bar{t}}$ system are also measured to help in understanding the PDFs. The angular difference in the transverse plane between the top and anti-top quarks is provided to compare to predictions of new physics beyond the standard model [16]. In addition, the normalized $\mathrm{t\bar{t}}$ cross sections are measured as a function of the transverse momenta of the top quark and of the top quark pair.

2 The CMS detector and simulation

2.1 The CMS detector

The central feature of the CMS apparatus is a superconducting solenoid of 6 m internal diameter, providing a magnetic field of 3.8 T. The solenoid volume encases the silicon pixel and strip tracker, a lead tungstate crystal electromagnetic calorimeter, and a brass and scintillator hadron calorimeter, each composed of a barrel and two endcap sections. Forward calorimeters extend the pseudorapidity (η) coverage provided by the barrel and endcap detectors. Muons are detected in gas-ionization chambers embedded in the steel flux-return yoke outside the solenoid. A more detailed description of the CMS detector, together with a definition of the coordinate system used and the relevant kinematic variables, can be found in ref. [17]. The particle-flow (PF) algorithm [18] is used to reconstruct objects in the event, combining information from all the CMS subdetectors. The missing transverse momentum vector ($\vec{p}_{\mathrm{T}}^{\,\mathrm{miss}}$) is defined as the projection onto the plane perpendicular to the beam axis of the negative vector sum of the momenta of all PF candidates in an event [19]. Its magnitude is referred to as $p_{\mathrm{T}}^{\mathrm{miss}}$.

2.2 Signal and background simulation

Monte Carlo (MC) techniques are used to simulate the $\mathrm{t\bar{t}}$ signal and the background processes. We use the POWHEG (v2) [20–23] generator to model the nominal $\mathrm{t\bar{t}}$ signal at

JHEP04(2018)060

next-to-leading order (NLO). In order to simulate $t\bar{t}$ events with additional partons, MadGraph5_aMC@NLO (v2.2.2) [24] (MG5_aMC@NLO) is used, which includes both leading-order (LO) and NLO matrix elements (MEs). Parton shower (PS) simulation is performed with Pythia8 (v8.205) [25], using the tune CUETP8M1 [26] to model the underlying event. Up to two partons in addition to the $t\bar{t}$ pair are calculated at NLO and combined with the Pythia8 PS simulation using the FXFX [27] algorithm, denoted as MG5_aMC@NLO+Pythia8[FXFX]. Up to three partons are considered at LO and combined with the Pythia8 PS simulation using the MLM [28] algorithm, denoted as MG5_aMC@NLO+Pythia8[MLM]. The data are also compared to predictions obtained with powheg samples interfaced with Herwig++ [29] (v 2.7.1) using the tune EE5C [30]. The signal samples are simulated assuming a top quark mass of 172.5 GeV and normalized to the inclusive cross section calculated at NNLO precision with next-to-next-to-leading-logarithmic (NNLL) accuracy [31].

For the simulation of W boson production and the Drell-Yan process, the MG5_aMC@NLO generator is used, and the samples are normalized to the cross sections calculated at NNLO [32]. The t-channel single top quark production in the tW channel is simulated with the powheg generator based on the five-flavor scheme [33, 34], and normalized to the cross sections calculated at NNLO [35]. Diboson samples (WW, WZ, and ZZ) are simulated at LO using Pythia8, and normalized to the cross section calculated at NNLO for the WW sample [36] and NLO for the WZ and ZZ samples [37].

The detector response to the final-state particles is simulated using Geant4 [38, 39]. Additional pp collisions in the same or nearby beam crossings (pileup) are also simulated with Pythia8 and superimposed on the hard-scattering events using a pileup multiplicity distribution that reflects that of the analyzed data. Simulated events are reconstructed and analyzed with the same software used to process the data.

3 Object and event selection

The dilepton final state of the $t\bar{t}$ decay consists of two leptons (electrons or muons), at least two jets, and $p_{\mathrm{T}}^{\mathrm{miss}}$ from the two neutrinos. Events are selected using dilepton triggers with asymmetric p_{T} thresholds. The low transverse momentum (p_{T}) threshold is 8 GeV for the muon and 12 GeV for the electron, and the high-p_{T} threshold is 17 GeV for both muon and electron. The trigger efficiency is measured in data using triggers based on $p_{\mathrm{T}}^{\mathrm{miss}}$ [40].

The reconstructed and selected muons [41] and electrons [42] are required to have $p_{\mathrm{T}} > 20$ GeV and $|\eta| < 2.4$. Since the primary leptons that originated from top quark decays are expected to be isolated, an isolation criterion is placed on each lepton to reduce the rate of secondary leptons from non-top hadronic decays. A relative isolation parameter is used, which is calculated as the sum of the p_{T} of charged and neutral hadrons and photons in a cone of angular radius $\Delta R = \sqrt{(\Delta\phi)^2 + (\Delta\eta)^2}$ around the direction of the lepton, divided by the lepton p_{T}, where $\Delta\phi$ and $\Delta\eta$ are the azimuthal and pseudorapidity differences, respectively, between the directions of the lepton and the other particle. Any mismodeling of the lepton selection in the simulation is accounted for by applying corrections derived using a "tag-and-probe" technique based on control regions in data [43].

JHEP04(2018)060

Dilepton	Selected	Reconstructed $t\bar{t}$ system
$t\bar{t}$-signal	11565 ± 14.19	10611 ± 13.61
$t\bar{t}$-others	6060 ± 10.28	4856 ± 9.24
Single top	869 ± 7.93	540 ± 6.32
Dibonson	73 ± 3.91	39 ± 2.87
W + jets	23 ± 10.84	36 ± 16.93
$Z/\gamma* \to \ell^+\ell^-$	507 ± 12.86	324 ± 10.75
MC total	19100 ± 25.85	16409 ± 26.85
Data	18891	16325

Table 1. The expected and observed numbers of events after selection are listed in the second column. The third column shows the numbers of reconstructed $t\bar{t}$ events.

Jets are reconstructed using PF candidates as inputs to the anti-k_T jet clustering algorithm [44, 45], with $\Delta R = 0.4$. The momenta of jets are corrected to account for effects from pileup, as well as nonuniformity and nonlinearity of the detector. For the data, energy corrections are also applied to correct the detector response [46]. We select jets with $p_T > 30\,\text{GeV}$ and $|\eta| < 2.4$ that pass identification criteria designed to reject noise in the calorimeters.

Jets from the hadronization of b quarks (b jets) are identified by the combined secondary vertex b tagging algorithm [47]. The jets are selected using a loose working point [48], corresponding to an efficiency of about 80% and a light-flavor jet rejection probability of 85%. The b tagging efficiency in the simulation is corrected to be consistent with that in data.

Events are required to have exactly two oppositely charged leptons with the invariant mass of the dilepton system $M_{\ell^+\ell^-} > 20\,\text{GeV}$, and two or more jets, at least one of which has to be identified as a b jet. For the same-flavor lepton channels (ee and $\mu\mu$), additional selection criteria are applied to reject events from Drell-Yan production: $p_T^{\text{miss}} > 40\,\text{GeV}$ and $|M_{\ell^+\ell^-} - M_Z| > 15\,\text{GeV}$, where M_Z is the Z boson mass [49]. The selected numbers of events after the selection are listed in table 1.

4 Signal definition

The measurements of normalized $t\bar{t}$ differential cross sections are performed at both particle and parton levels as a function of kinematic observables, defined at the generator level. The particle-level top quark is defined at the generator level using the procedure described below. This approach avoids theoretical uncertainties in the measurements due to the different calculations within each generator, and leads to results that are largely independent of the generator implementation and tuning. Top quarks are reconstructed in the simulation starting from the final-state particles with a mean lifetime greater than 30 ps at the generator level, as summarized in table 2.

JHEP04(2018)060

Object	Definition	Selection criteria
Neutrino	neutrinos not from hadron decays	none
Dressed lepton	anti-k_T algorithm with $\Delta R = 0.1$ using electrons, muons, and photons not from hadron decays	$p_T > 20\,\text{GeV}$, $\lvert\eta\rvert < 2.4$
b quark jet	anti-k_T algorithm with $\Delta R = 0.4$ using all particles and ghost-B hadrons not including any neutrinos nor particles used in dressed leptons	$p_T > 30\,\text{GeV}$, $\lvert\eta\rvert < 2.4$ with ghost-B hadrons

Table 2. Summary of the object definitions at the particle level.

Leptons are "dressed", which means that leptons are defined using the anti-k_T clustering algorithm [44, 45] with $\Delta R = 0.1$ to account for final-state radiated photons. To avoid the ambiguity of additional leptons at the generator level, the clustering is applied to electrons, muons, and photons not from hadron decays. Events with leptons associated with τ lepton decays are treated as background. Leptons are required to satisfy the same acceptance requirements as imposed on the reconstructed objects described in section 3, i.e., $p_T > 20\,\text{GeV}$ and $|\eta| < 2.4$.

The generator-level jets are clustered using the anti-k_T algorithm with $\Delta R = 0.4$. The clustering is applied to all final-state particles except neutrinos and particles already included in the dressed-lepton definition. Jets are required to have $p_T > 30\,\text{GeV}$ and $|\eta| < 2.4$ to be consistent with the reconstructed-object selection. To identify the bottom quark flavor of the jet, the ghost-B hadron technique [13] is used in which short-lifetime B hadrons are included in the jet clustering after scaling down their momentum to be negligible. A jet is identified as a b jet if it contains any B hadrons among its constituents.

A W boson at the particle level is defined by combining a dressed lepton and a neutrino. In each event, a pair of particle-level W bosons is chosen among the possible combinations such that the sum of the absolute values of the invariant mass differences with respect to the W boson mass is minimal [49]. Similarly, a top quark at the particle level is defined by combining a particle-level W boson and a b jet. The combination of a W boson and a b jet with the minimum invariant mass difference from the correct top quark mass [49] is selected. Events are considered to be in the visible phase space if they contain a pair of particle-level top quarks, constructed from neutrinos, dressed leptons, and b jets. Simulated dilepton events that are not in the visible phase space are considered as background and combined with the non-dilepton $t\bar{t}$ decay background contribution, subsequently denoted as $t\bar{t}$-others.

In addition, the top quark and $t\bar{t}$ system observables are defined before the top quark decays into a bottom quark and a W boson and after QCD radiation, which we refer to as the parton level. The $t\bar{t}$ system at the parton level is calculated in the generator at NLO. The normalized differential cross sections at the parton level are derived by extrapolating the measurements into the full phase space, which includes the experimentally inaccessible regions, such as at high rapidity and low transverse momentum of the leptons and jets.

JHEP04(2018)060

5 Reconstruction of the $\mathrm{t\bar{t}}$ system

The top quark reconstruction method is adopted from the recent CMS measurement of the differential $\mathrm{t\bar{t}}$ cross section [4]. In the dilepton channel, the reconstruction of the neutrino and antineutrino is crucial in measuring the top quark kinematic observables. Using an analytical approach [50, 51], the six unknown neutrino degrees of freedom are constrained by the two measured components of $\vec{p}_{\mathrm{T}}^{\,\mathrm{miss}}$ and the assumed invariant masses of both the W boson and top quark. The efficiency for finding a physical solution depends on the detector resolution, which is accounted for by reconstructing the $\mathrm{t\bar{t}}$ system in both the MC simulation and data with 100 trials, using random modifications of the measured leptons and b jets within their resolution functions. The efficiency for finding a physical solution to the kinematic reconstruction is approximately 90%, as determined from simulation and data. The numbers of events remaining after reconstructing the ttbar system are listed in table 1.

In each trial, the solution with the minimum invariant mass of the $\mathrm{t\bar{t}}$ system is selected, and a weight is calculated based on the expected invariant mass distribution of the lepton and b jet pairs ($M_{\ell\mathrm{b}}$) at generator level. The lepton and b jet pairs with the maximum sum of weights are chosen for the final solution of the $\mathrm{t\bar{t}}$ system, and the reconstructed neutrino momentum is taken from the weighted average over the trials.

The kinematic variables of the leptons, b jets, top quarks, and $\mathrm{t\bar{t}}$ system are taken from the selected final solution. Figure 1 shows the distributions of the transverse momenta of leptons ($p_{\mathrm{T}}^{\mathrm{lep}}$), jets ($p_{\mathrm{T}}^{\mathrm{jet}}$), and top quarks ($p_{\mathrm{T}}^{\mathrm{t}}$), and the rapidity of the top quarks (y^{t}). Figure 2 displays the distributions of the transverse momentum ($p_{\mathrm{T}}^{\mathrm{t\bar{t}}}$), rapidity ($y^{\mathrm{t\bar{t}}}$), and invariant mass ($M^{\mathrm{t\bar{t}}}$) of the $\mathrm{t\bar{t}}$ system, and the azimuthal angle between the top quarks ($\Delta\phi^{\mathrm{t\bar{t}}}$). In the upper panel of each figure, the data points are compared to the sum of the expected contributions obtained from MC simulated events reconstructed as the data. The lower panel shows the ratio of the data to the expectations. The measured $p_{\mathrm{T}}^{\mathrm{lep}}$, $p_{\mathrm{T}}^{\mathrm{jet}}$, and $p_{\mathrm{T}}^{\mathrm{t}}$ distributions are softer than those predicted by the MC simulation, resulting in the negative slopes observed in the bottom panels. However, in general, there is reasonable agreement between the data and simulation within the uncertainties, which are discussed in section 7.

6 Normalized differential cross sections

The normalized differential $\mathrm{t\bar{t}}$ cross sections $(1/\sigma)(\mathrm{d}\sigma/\mathrm{d}X)$ are measured as a function of several different kinematic variables X. The variables include $p_{\mathrm{T}}^{\mathrm{t}}$, $p_{\mathrm{T}}^{\mathrm{t\bar{t}}}$, y^{t}, $y^{\mathrm{t\bar{t}}}$, $M^{\mathrm{t\bar{t}}}$, and $\Delta\phi^{\mathrm{t\bar{t}}}$, at both the particle and parton levels. In addition, the measurements are performed with $p_{\mathrm{T}}^{\mathrm{lep}}$ and $p_{\mathrm{T}}^{\mathrm{jet}}$ at the particle level. The measurements are compared to the predictions of POWHEG+PYTHIA8, MG5_aMC@NLO+PYTHIA8[FXFX], MG5_aMC@NLO+PYTHIA8[MLM], and POWHEG+HERWIG++.

The non-$\mathrm{t\bar{t}}$ backgrounds are estimated from simulation and subtracted from the data. For Drell-Yan processes the normalization of the simulation is determined from the data using the "$R_{\mathrm{out/in}}$" method [52–54]. The non-$\mathrm{t\bar{t}}$ backgrounds are first subtracted from the

JHEP04(2018)060

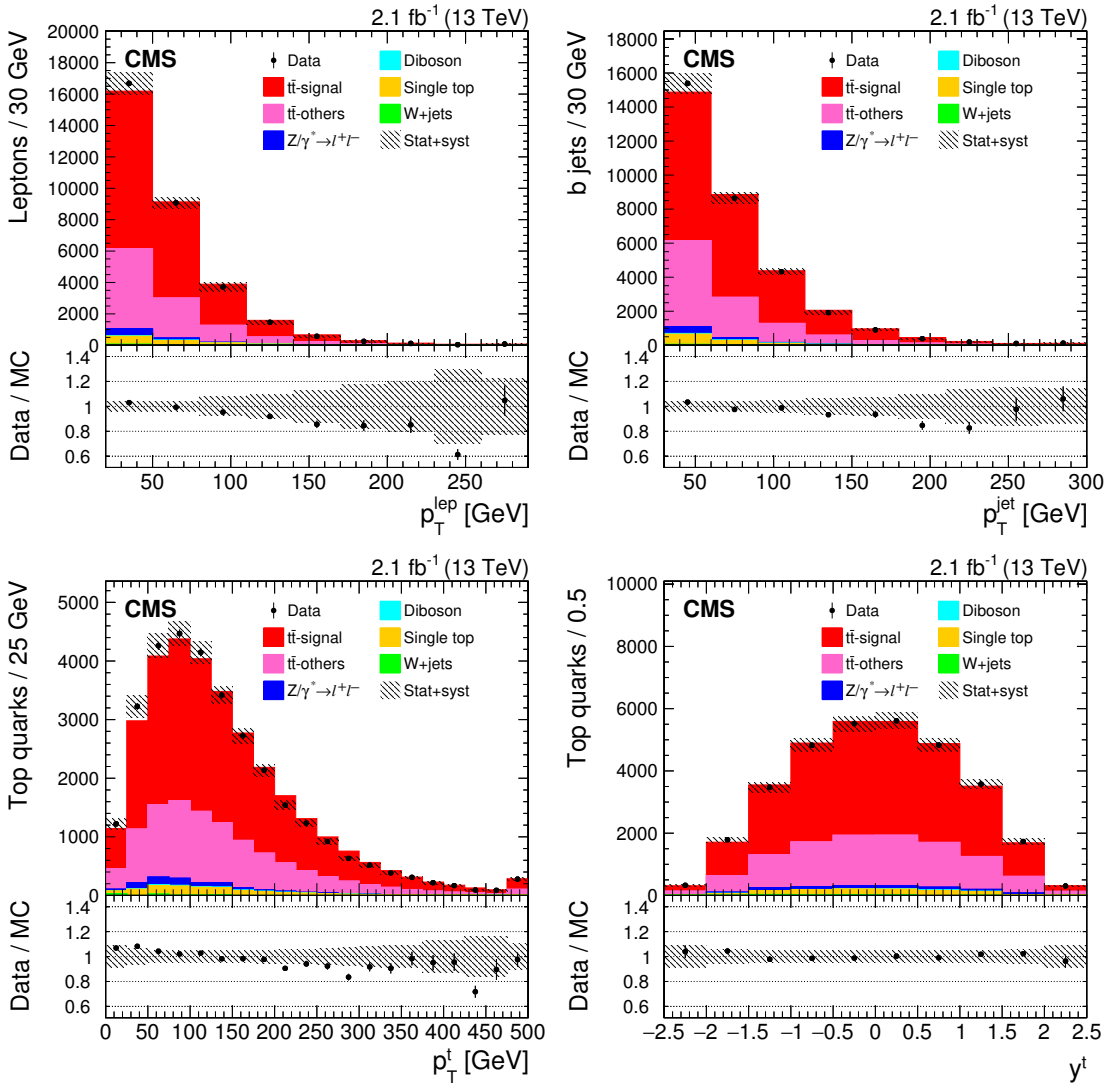

Figure 1. Reconstructed $p_{\mathrm{T}}^{\mathrm{lep}}$ (upper left), $p_{\mathrm{T}}^{\mathrm{jet}}$ (upper right), $p_{\mathrm{T}}^{\mathrm{t}}$ (lower left), and y^{t} (lower right) distributions from data (points) and from MC simulation (shaded histograms). The signal definition for particle level is considered to distinguish $\mathrm{t\bar{t}}$-signal and $\mathrm{t\bar{t}}$-others. All corrections described in the text are applied to the simulation. The last bin includes the overflow events. The uncertainties shown by the vertical bars on the data points are statistical only while the hatched band shows the combined statistical and systematic uncertainties added in quadrature. The lower panels display the ratios of the data to the MC prediction.

JHEP04(2018)060

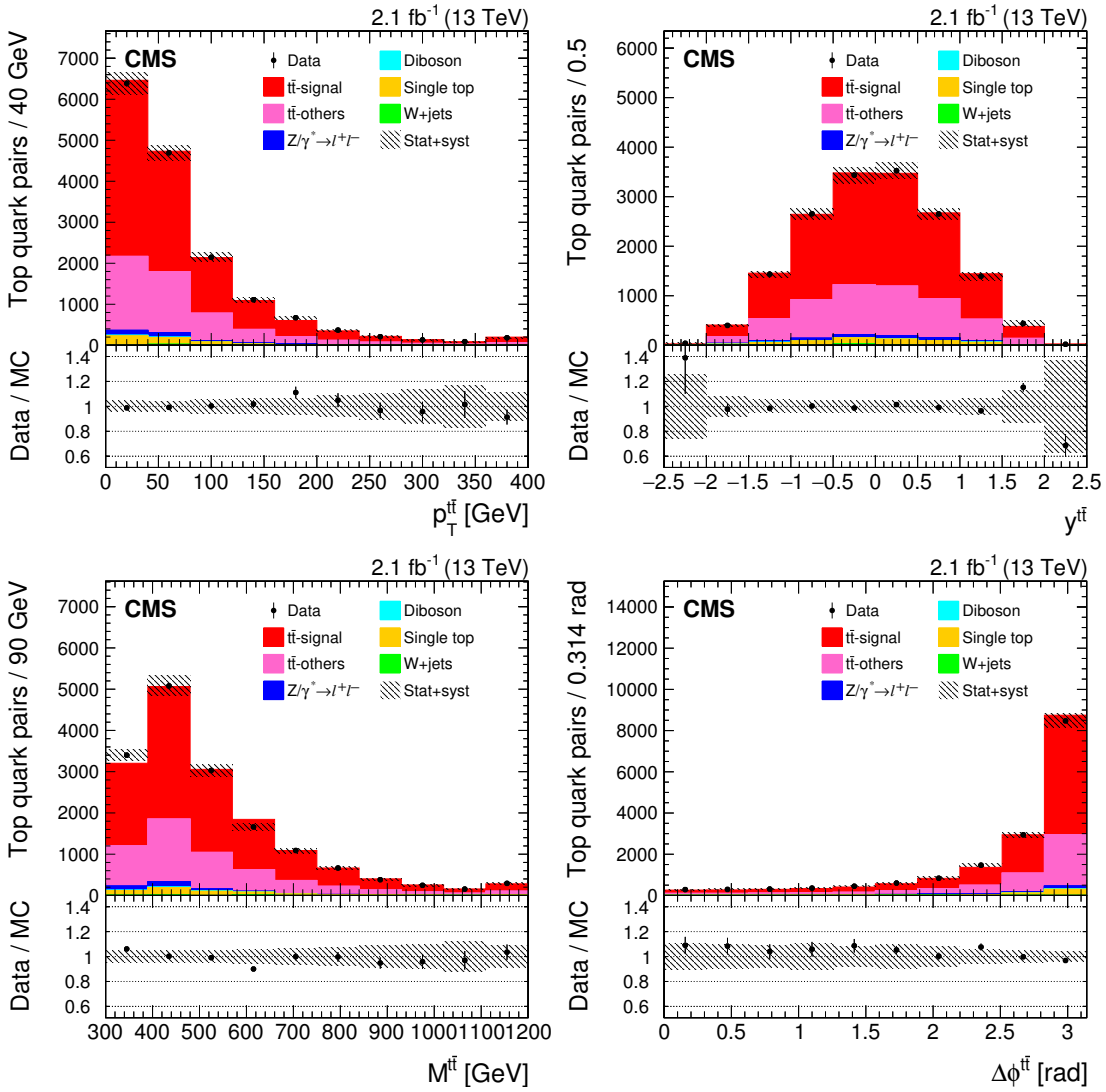

Figure 2. Reconstructed $p_{\mathrm{T}}^{\mathrm{t\bar{t}}}$ (upper left), $y^{\mathrm{t\bar{t}}}$ (upper right), $M^{\mathrm{t\bar{t}}}$ (lower left), and $\Delta\phi^{\mathrm{t\bar{t}}}$ (lower right) distributions from data (points) and from MC simulation (shaded histograms). The signal definition for particle level is considered to distinguish $\mathrm{t\bar{t}}$-signal and $\mathrm{t\bar{t}}$-others. All corrections described in the text are applied to the simulation. The last bin includes the overflow events. The uncertainties shown by the vertical bars on the data points are statistical only while the hatched band shows the combined statistical and systematic uncertainties added in quadrature. The lower panels display the ratios of the data to the MC prediction.

JHEP04(2018)060

measured distributions. The data distributions are slightly lower than those from the MC simulation. The $\mathrm{t\bar{t}}$-others backgrounds are then removed as a proportion of the total $\mathrm{t\bar{t}}$ contribution by applying a single correction factor k shown in eq. (6.1), using eq. (6.2):

$$k = \frac{N^{\mathrm{data}} - N^{\mathrm{MC}}_{\mathrm{non\text{-}t\bar{t}}}}{N^{\mathrm{MC}}_{\mathrm{t\bar{t}\text{-}sig}} + N^{\mathrm{MC}}_{\mathrm{t\bar{t}\text{-}others}}}, \tag{6.1}$$

$$N^{\mathrm{data}}_{\mathrm{t\bar{t}\text{-}sig}} = N^{\mathrm{data}} - N^{\mathrm{MC}}_{\mathrm{non\text{-}t\bar{t}}} - kN^{\mathrm{MC}}_{\mathrm{t\bar{t}\text{-}others}}. \tag{6.2}$$

Here, $N^{\mathrm{MC}}_{\mathrm{non\text{-}t\bar{t}}}$ is the total estimate for the non-$\mathrm{t\bar{t}}$ background from the MC simulation, $N^{\mathrm{MC}}_{\mathrm{t\bar{t}\text{-}sig}}$ is the total MC-predicted $\mathrm{t\bar{t}}$ signal yield, and $N^{\mathrm{MC}}_{\mathrm{t\bar{t}\text{-}others}}$ is the total MC prediction of the remaining $\mathrm{t\bar{t}}$ background. The $\mathrm{t\bar{t}}$ signal yield, $N^{\mathrm{data}}_{\mathrm{t\bar{t}\text{-}sig}}$, is then extracted from the number of data events, N^{data}, separately in each bin of the kinematic distributions, as shown in eq. (6.2).

The bin widths of the distributions are chosen to control event migration between the bins at the reconstruction and generator level due to detector resolutions. We define the purity (stability) as the number of events generated and correctly reconstructed in a certain bin, divided by the total number of events in the reconstruction-level (generator-level) bin. The bin widths are chosen to give both a purity and a stability of about 50%.

Detector resolution and reconstruction efficiency effects are corrected using an unfolding procedure. The method relies on a response matrix that maps the expected relation between the true and reconstructed variables taken from the POWHEG+PYTHIA8 simulation. The D'Agostini method [55] is employed to perform the unfolding. The effective regularization strength of the iterative D'Agostini unfolding is controlled by the number of iterations. A small number of iterations can bias the measurement towards the simulated prediction, while with a large number of iterations the result converges to that of a matrix inversion. The number of iterations is optimized for each distribution, using simulation to find the minimum number of iterations that reduces the bias to a negligible level. This optimization is performed with the multiplication of the response matrix and does not require any regularization. A detailed description of the method can be found in ref. [13].

7 Systematic uncertainties

Several sources of systematic uncertainties are studied. The normalized differential cross sections are remeasured with respect to each source of systematic uncertainty individually, and the differences from the nominal values in each bin are taken as the corresponding systematic uncertainty. The overall systematic uncertainties are then obtained as the quadratic sum of the individual components.

The pileup distribution used in the simulation is varied by shifting the assumed total inelastic pp cross section by $\pm 5\%$, in order to determine the associated systematic uncertainty. The systematic uncertainties in the lepton trigger, identification, and isolation efficiencies are determined by varying the measured scale factors by their total uncertainties. Uncertainties coming from the jet in the jet energy scale (JES) and jet energy resolution (JER) are determined on a per-jet basis by shifting the energies of the jets [56]

JHEP04(2018)060

within their measured energy scale and resolution uncertainties. The b tagging uncertainty is estimated by varying its efficiency uncertainty.

The uncertainty in the non-$\mathrm{t\bar{t}}$ background normalization is estimated using a 15–30% variation in the background yields, which is based on a previous CMS measurement of the $\mathrm{t\bar{t}}$ cross section [40]. The uncertainty in the shape of the $\mathrm{t\bar{t}}$-others contribution is obtained by reweighting the p_{T} distribution of the top quark for the $\mathrm{t\bar{t}}$-others events to match the data and comparing with the unweighted contribution. For the theoretical uncertainties, we investigate the effect of the choice of PDFs, factorization and renormalization scales (μ_{F} and μ_{R}), variation of the top quark mass, top quark p_{T}, and hadronization and generator modeling.

The PDF uncertainty is estimated using the uncertainties in the NNPDF30_NLO_as_0118 set with the strong coupling strength $\alpha_{\mathrm{s}} = 0.118$ [57]. We measure 100 individual uncertainties and take the root-mean-square as the PDF uncertainty, following the PDF4LHC recommendation [58]. In addition, we consider the PDF sets with $\alpha_{\mathrm{s}} = 0.117$ and 0.119. The MC generator modeling uncertainties are estimated by taking the difference between the results based on the POWHEG and MG5_aMC@NLO generators.

The uncertainty from the choice of μ_{F} and μ_{R} is estimated by varying the scales by a factor of two up and down in POWHEG independently for the ME and PS steps. For the ME calculation, all possible combinations are considered independently, excluding the most extreme cases of $(\mu_{\mathrm{F}}, \mu_{\mathrm{R}}) = (0.5, 2)$ and $(2, 0.5)$ [59, 60]. The scale uncertainty in the PS modeling is assessed using dedicated MC samples with the scales varied up and down together. The uncertainties in the factorization and renormalization scales in the ME and PS calculations are taken as the envelope of the differences with respect to the nominal parameter choice.

We evaluate the top quark mass uncertainty by taking the maximum deviation between the nominal MC sample with a top quark mass of 172.5 GeV and samples with masses of 171.5 and 173.5 GeV. The $\mathrm{t\bar{t}}$ signal cross sections are not corrected for the mismodeling of the top quark p_{T} distribution in simulation. Instead, a systematic uncertainty from this mismodeling is obtained by comparing the nominal results to the results obtained from a response matrix using $\mathrm{t\bar{t}}$-signal in which the top quark p_{T} distribution is reweighted to match the data. The uncertainty from hadronization and PS modeling is estimated by comparing the results obtained from POWHEG samples interfaced with PYTHIA8 and with HERWIG++.

Table 3 lists typical values for the statistical and systematic uncertainties in the measured normalized $\mathrm{t\bar{t}}$ differential cross sections. The table gives the uncertainty sources and corresponding range of the median uncertainty of each distribution, at both the particle and parton levels. The hadronization is the dominant systematic uncertainty source for $p_{\mathrm{T}}^{\mathrm{t}}$ (4.9% at particle and 7.1% at parton level) and $M^{\mathrm{t\bar{t}}}$ (5.9% at particle and 7.4% at parton level), and the MC generator modeling is dominant for y^{t} (2.3% at particle and 2.2% at parton level), $p_{\mathrm{T}}^{\mathrm{t\bar{t}}}$ (6.1% at particle and 3.9% at parton level), $y^{\mathrm{t\bar{t}}}$ (1.2% at particle and 1.6% at parton level), and $\Delta\phi^{\mathrm{t\bar{t}}}$ (9.2% at particle and 7.3% at parton level). In general, the MC generator modeling and hadronization are the dominant systematic uncertainty sources for both the particle- and parton-level measurements.

JHEP04(2018)060

Uncertainty source	Particle level [%]	Parton level [%]
Statistical	0.24–0.59	0.36–0.63
Pileup modeling	0.02–0.48	0.07–0.49
Trigger efficiency	0.03–0.67	0.06–0.82
Lepton efficiency	0.06–0.94	0.07–0.90
JES	0.14–2.04	0.29–1.44
JER	0.04–0.85	0.29–0.65
b jet tagging	0.12–1.19	0.26–1.16
Background	0.13–2.14	0.09–1.28
PDFs	0.15–0.96	0.17–0.97
MC generator	0.66–9.24	1.61–7.32
Fact./renorm.	0.10–4.15	0.17–4.15
Top quark mass	0.49–1.89	0.68–3.05
Top quark p_{T}	0.02–1.74	0.02–0.69
Hadronization — PS modeling	0.70–5.85	0.41–7.44
Total systematic uncertainty	1.7–15	3.1–13

Table 3. Statistical and systematic uncertainties in the normalized $\mathrm{t\bar{t}}$ differential cross sections at particle and parton levels. The uncertainty sources and the corresponding range of the median uncertainty of each distribution are shown in percent.

8 Results

The normalized differential $\mathrm{t\bar{t}}$ cross sections are measured by subtracting the background contribution, correcting for detector effects and acceptance, and dividing the resultant number of $\mathrm{t\bar{t}}$ signal events by the total inclusive $\mathrm{t\bar{t}}$ cross section. Figures 3 and 4 show the normalized differential $\mathrm{t\bar{t}}$ cross sections as a function of $p_{\mathrm{T}}^{\mathrm{lep}}$, $p_{\mathrm{T}}^{\mathrm{jet}}$, $p_{\mathrm{T}}^{\mathrm{t}}$, y^{t}, $p_{\mathrm{T}}^{\mathrm{t\bar{t}}}$, $y^{\mathrm{t\bar{t}}}$, $M^{\mathrm{t\bar{t}}}$, and $\Delta\phi^{\mathrm{t\bar{t}}}$ at the particle level in the visible phase space. Parton-level results are also independently extrapolated to the full phase space using the POWHEG+PYTHIA8 $\mathrm{t\bar{t}}$ simulation. Figures 5 and 6 show the normalized differential $\mathrm{t\bar{t}}$ cross sections as a function of $p_{\mathrm{T}}^{\mathrm{t}}$, y^{t}, $p_{\mathrm{T}}^{\mathrm{t\bar{t}}}$, $y^{\mathrm{t\bar{t}}}$, $M^{\mathrm{t\bar{t}}}$, and $\Delta\phi^{\mathrm{t\bar{t}}}$ at parton level in the full phase space. The measured data are compared to different standard model predictions from POWHEG+PYTHIA8, MG5_aMC@NLO+PYTHIA8[FXFX], MG5_aMC@NLO+PYTHIA8[MLM], and POWHEG+HERWIG++ in the figures. The values of the measured normalized differential $\mathrm{t\bar{t}}$ cross sections at the parton and particle levels with their statistical and systematic uncertainties are listed in appendices A and B.

The compatibility between the measurements and the predictions is quantified by means of a χ^2 test performed with the full covariance matrix from the unfolding procedure, including the systematic uncertainties. Tables 4 and 5 report the values obtained for the χ^2 with the numbers of degrees of freedom (dof) and the corresponding p-values [61]. The lepton, jet, and top quark p_{T} spectra in data tend to be softer than the MC predictions for the high-p_{T} region. A similar trend was also observed at $\sqrt{s} = 8\,\mathrm{TeV}$ by both the ATLAS

JHEP04(2018)060

and CMS experiments [4, 5]. The POWHEG+PYTHIA8 generator better describes the $p_{\mathrm{T}}^{\mathrm{t\bar{t}}}$, y^{t}, and $y^{\mathrm{t\bar{t}}}$ distributions at the particle and parton levels, while POWHEG+HERWIG++ is found to be in good agreement for the $p_{\mathrm{T}}^{\mathrm{t}}$ at the parton and particle levels. In general, measurements are found to be in fair agreement with predictions within the uncertainties.

The parton-level results are also compared to the following perturbative QCD calculations:

- An approximate NNLO calculation based on QCD threshold expansions beyond the leading-logarithmic approximation using the CT14nnlo PDF set [62].
- An approximate next-to-NNLO ($\mathrm{N^3LO}$) calculation performed with the resummation of soft-gluon contributions in the double-differential cross section at NNLL accuracy in momentum space using the MMHT2014 PDF set [63, 64].
- An improved NNLL QCD calculation (NLO+NNLL') [65] with simultaneous resummation of soft and small-mass logarithms to NNLL accuracy, matched with both the standard soft-gluon resummation at NNLL accuracy and the fixed-order calculation at NLO accuracy, using the MTSW2008nnlo PDF set.
- A full NNLO calculation based on the NNPDF3.0 PDF set [66].

The measurements and the perturbative QCD predictions are shown in figures 7 and 8. Table 6 gives the χ^2/dof and the corresponding p-values for the agreement between the measurements and QCD calculations. The normalized differential $\mathrm{t\bar{t}}$ cross sections as a function of the y^{t}, $y^{\mathrm{t\bar{t}}}$, and $p_{\mathrm{T}}^{\mathrm{t\bar{t}}}$ are found to be in good agreement with the different predictions considered. We observe some tension between the data and the NNLO predictions for other variables such as the $p_{\mathrm{T}}^{\mathrm{t}}$ and $M^{\mathrm{t\bar{t}}}$.

9 Summary

The normalized differential cross sections for top quark pair production have been presented by the CMS experiment in the dilepton decay channel in pp collisions at $\sqrt{s} = 13\,\mathrm{TeV}$ with data corresponding to an integrated luminosity of $2.1\,\mathrm{fb}^{-1}$. The differential cross sections are measured as a function of several kinematic variables at particle level in a visible phase space corresponding to the detector acceptance and at parton level in the full phase space. The measurements are compared to the predictions from Monte Carlo simulations and calculations in perturbative quantum chromodynamics. In general, the measurements are in fairly good agreement with predictions. We confirm that the top quark p_{T} spectrum in data is softer than the Monte Carlo predictions at both particle and parton levels, as reported by the ATLAS and CMS experiments. The present results are in agreement with the earlier ATLAS and CMS measurements. We also find that the measurements are in better agreement with calculations within quantum chromodynamics up to next-to-next-to-leading-order accuracy at the parton level compared to previous next-to-leading-order predictions.

JHEP04(2018)060

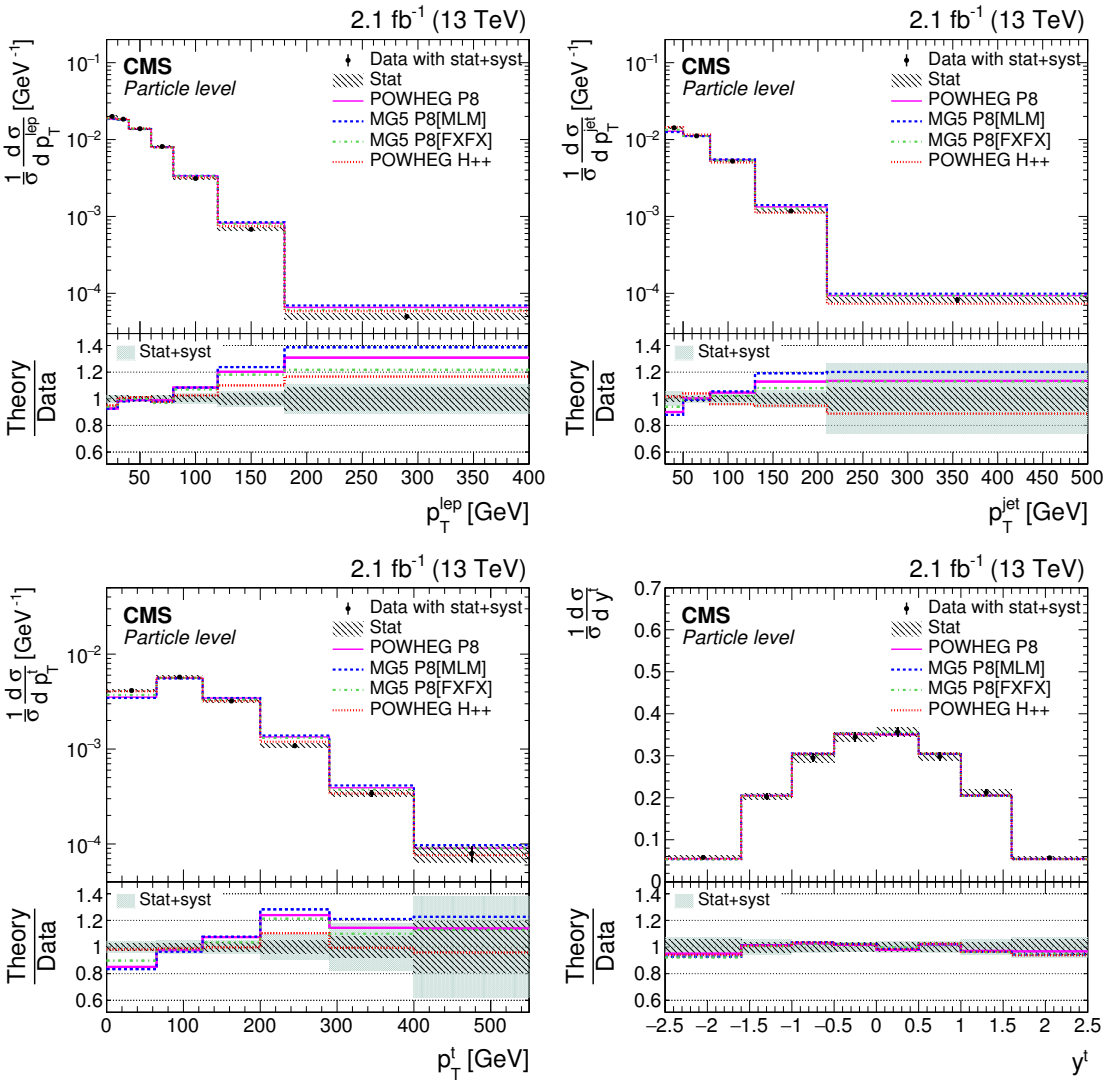

Figure 3. Normalized differential $t\bar{t}$ cross sections as a function of lepton (upper left), jet (upper right), and top quark p_T (lower left) and top quark rapidity (lower right), measured at the particle level in the visible phase space and combining the distributions for top quarks and antiquarks. The measured data are compared to different standard model predictions from POWHEG+PYTHIA8 (POWHEG P8), MG5_aMC@NLO+PYTHIA8[MLM] (MG5 P8[MLM]), MG5_aMC@NLO+PYTHIA8[FXFX] (MG5 P8[FXFX]), and POWHEG+HERWIG++ (POWHEG H++). The vertical bars on the data points indicate the total (combined statistical and systematic) uncertainties while the hatched band shows the statistical uncertainty. The lower panel gives the ratio of the theoretical predictions to the data. The light-shaded band displays the combined statistical and systematic uncertainties added in quadrature.

JHEP04(2018)060

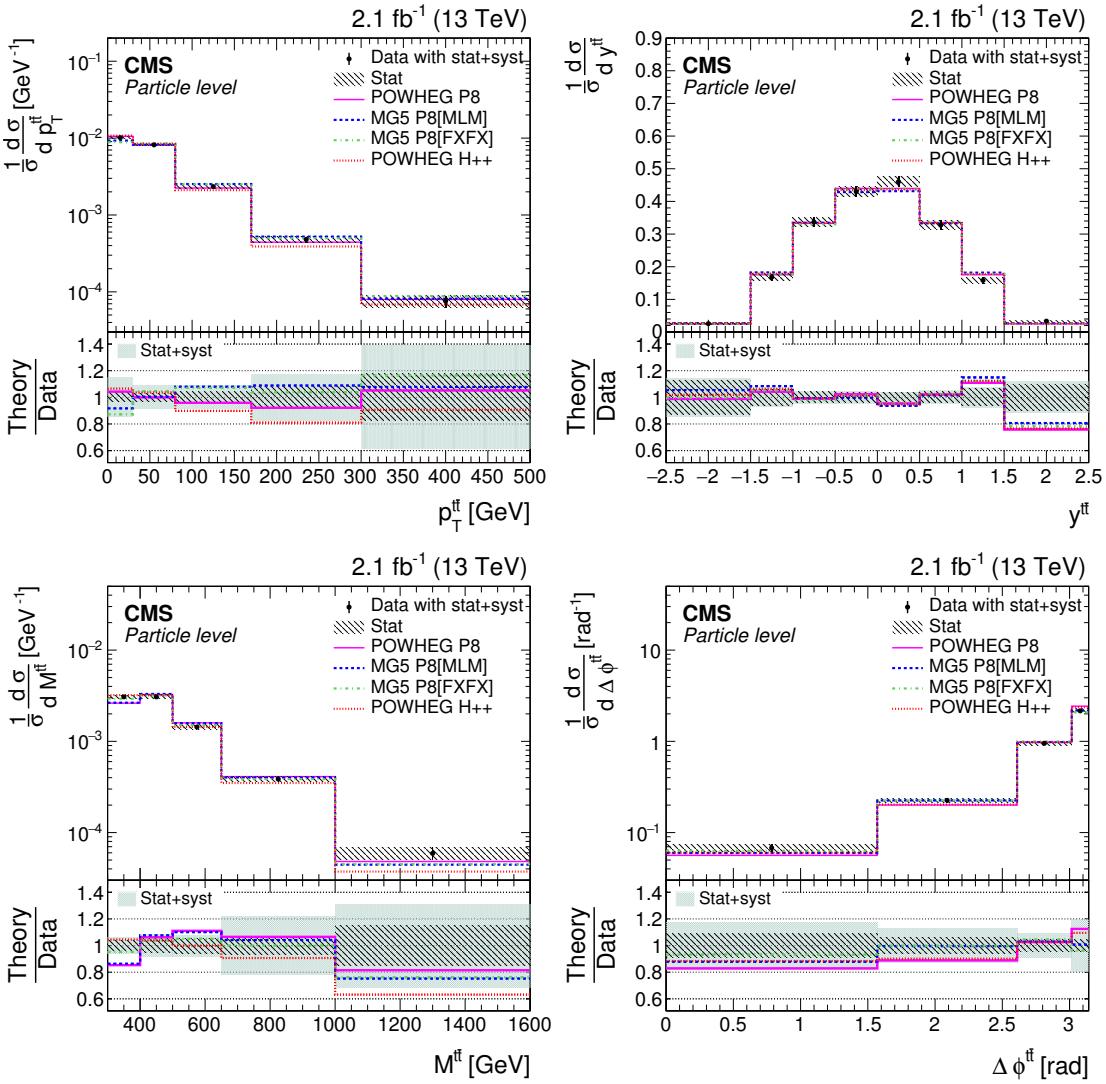

Figure 4. Normalized differential $\mathrm{t\bar{t}}$ cross sections as a function of $p_{\mathrm{T}}^{\mathrm{t\bar{t}}}$ (upper left), $y^{\mathrm{t\bar{t}}}$ (upper right), $M^{\mathrm{t\bar{t}}}$ (lower left), and $\Delta\phi^{\mathrm{t\bar{t}}}$ (lower right), measured at the particle level in the visible phase space. The measured data are compared to different standard model predictions from POWHEG+PYTHIA8 (POWHEG P8), MG5_aMC@NLO+PYTHIA8[MLM] (MG5 P8[MLM]), MG5_aMC@NLO+PYTHIA8[FXFX] (MG5 P8[FXFX]), and POWHEG+HERWIG++ (POWHEG H++). The vertical bars on the data points indicate the total (combined statistical and systematic) uncertainties while the hatched band shows the statistical uncertainty. The lower panel gives the ratio of the theoretical predictions to the data. The light-shaded band displays the combined statistical and systematic uncertainties added in quadrature.

JHEP04(2018)060

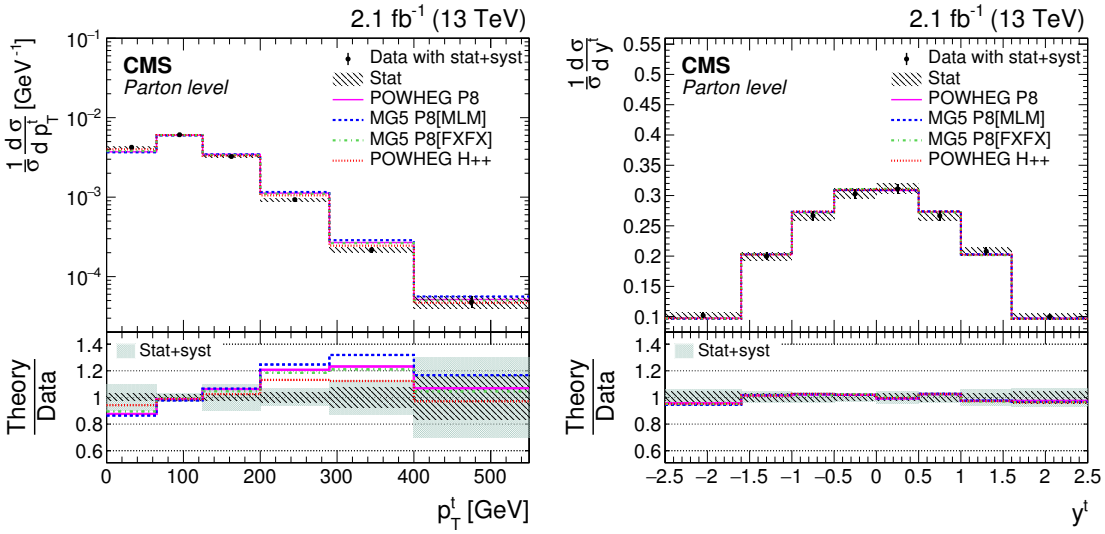

Figure 5. Normalized differential $\mathrm{t\bar{t}}$ cross sections as a function of top quark p_{T} (left) and top quark rapidity (right), measured at the parton level in the full phase space and combining the distributions for top quarks and antiquarks. The measured data are compared to different standard model predictions from POWHEG+PYTHIA8 (POWHEG P8), MG5_aMC@NLO+PYTHIA8[MLM] (MG5 P8[MLM]), MG5_aMC@NLO+PYTHIA8[FXFX] (MG5 P8[FXFX]), and POWHEG+HERWIG++ (POWHEG H++). The vertical bars on the data points indicate the total (combined statistical and systematic) uncertainties while the hatched band shows the statistical uncertainty. The lower panel gives the ratio of the theoretical predictions to the data. The light-shaded band displays the combined statistical and systematic uncertainties added in quadrature.

JHEP04(2018)060

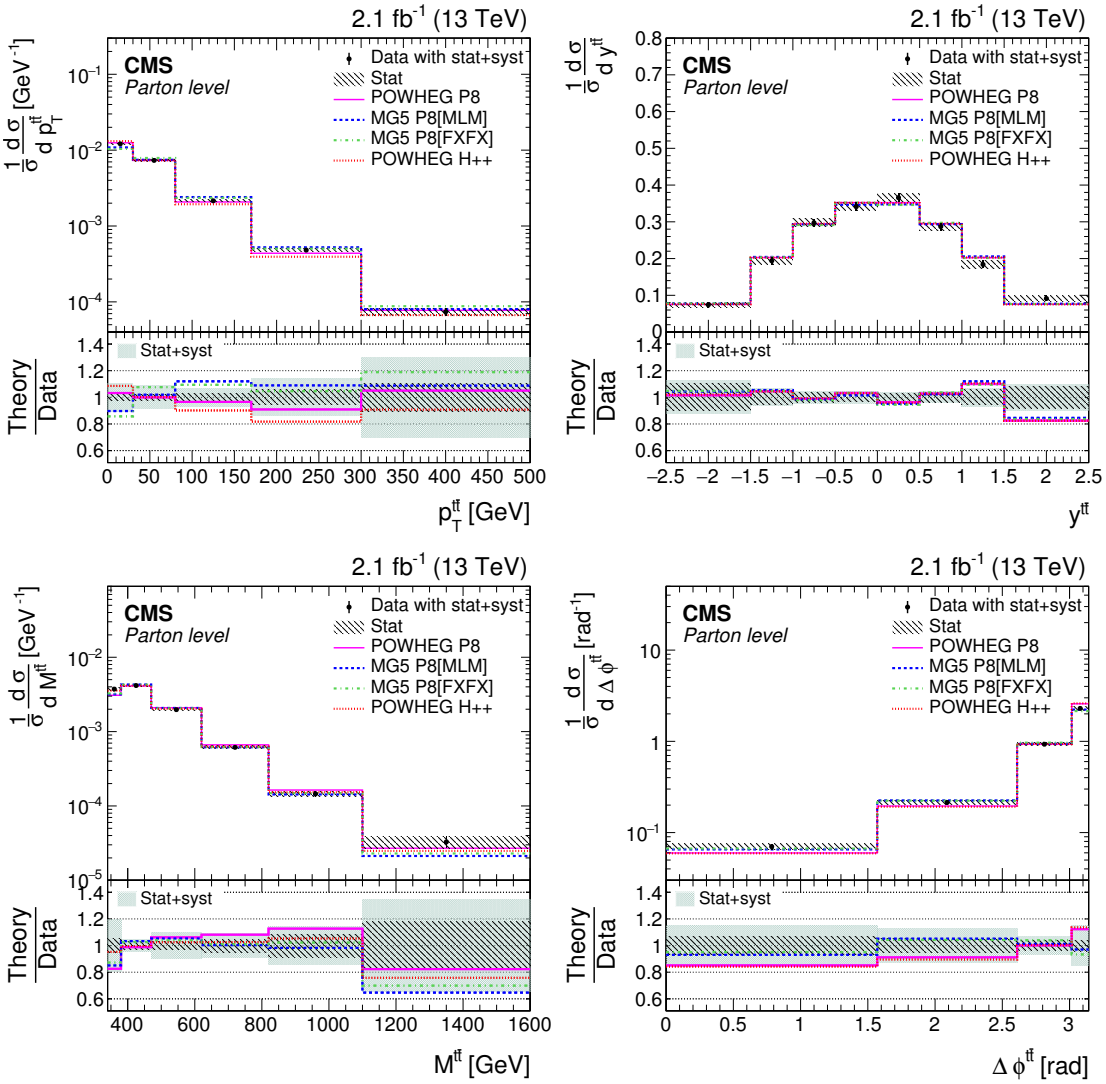

Figure 6. Normalized differential $\mathrm{t\bar{t}}$ cross sections as a function of $p_{\mathrm{T}}^{\mathrm{t\bar{t}}}$ (upper left), $y^{\mathrm{t\bar{t}}}$ (upper right), $M^{\mathrm{t\bar{t}}}$ (lower left), and $\Delta\phi^{\mathrm{t\bar{t}}}$ (lower right), measured at the parton level in the full phase space. The measured data are compared to different standard model predictions from POWHEG+PYTHIA8 (POWHEG P8), MG5_aMC@NLO+PYTHIA8[MLM] (MG5 P8[MLM]), MG5_aMC@NLO+PYTHIA8[FXFX] (MG5 P8[FXFX]), and POWHEG+HERWIG++ (POWHEG H++). The vertical bars on the data points indicate the total (combined statistical and systematic) uncertainties while the hatched band shows the statistical uncertainty. The lower panel gives the ratio of the theoretical predictions to the data. The light-shaded band displays the combined statistical and systematic uncertainties added in quadrature.

JHEP04(2018)060

	POWHEG + PYTHIA8		MG5_aMC@NLO + PYTHIA8 [MLM]		MG5_aMC@NLO + PYTHIA8 [FXFX]		POWHEG + HERWIG++	
Variable	χ^2/dof	p-value	χ^2/dof	p-value	χ^2/dof	p-value	χ^2/dof	p-value
p_T^{lep}	63.4/6	<0.01	79.5/6	<0.01	44.1/6	<0.01	20.2/6	<0.01
p_T^{jet}	32.4/4	<0.01	60.0/4	<0.01	10.8/4	0.029	11.1/4	0.03
p_T^t	57.2/5	<0.01	77.7/5	<0.01	31.6/5	<0.01	4.2/5	0.53
y^t	5.1/7	0.65	4.7/7	0.69	3.7/7	0.81	4.9/7	0.67
$p_T^{t\bar{t}}$	2.6/4	0.62	7.1/4	0.13	13.1/4	0.01	9.5/4	0.05
$y^{t\bar{t}}$	8.6/7	0.28	12.3/7	0.09	8.8/7	0.26	10.0/7	0.19
$M^{t\bar{t}}$	16.9/4	<0.01	16.5/4	<0.01	5.3/4	0.26	14.2/4	<0.01
$\Delta\phi^{t\bar{t}}$	14.7/3	<0.01	1.1/3	0.79	1.3/3	0.74	9.7/3	0.02

Table 4. The χ^2/dof and p-values for the comparison of the measured normalized $t\bar{t}$ differential cross sections with different model predictions at the particle level for each of the kinematic variables.

	POWHEG + PYTHIA8		MG5_aMC@NLO + PYTHIA8 [MLM]		MG5_aMC@NLO + PYTHIA8 [FXFX]		POWHEG + HERWIG++	
Variable	χ^2/dof	p-value	χ^2/dof	p-value	χ^2/dof	p-value	χ^2/dof	p-value
p_T^t	67.6/5	<0.01	99.1/5	<0.01	49.4/5	<0.01	19.0/5	<0.01
y^t	4.4/7	0.73	5.1/7	0.65	5.4/7	0.61	5.3/7	0.63
$p_T^{t\bar{t}}$	4.4/4	0.35	24.1/4	<0.01	38.7/4	<0.01	19.2/4	<0.01
$y^{t\bar{t}}$	7.7/7	0.36	9.2/7	0.24	9.3/7	0.23	8.0/7	0.33
$M^{t\bar{t}}$	21.2/5	<0.01	6.5/5	0.26	4.3/5	0.51	1.6/5	0.90
$\Delta\phi^{t\bar{t}}$	22.3/3	<0.01	1.7/3	0.65	3.9/3	0.28	27.9/3	<0.01

Table 5. The χ^2/dof and p-values for the comparison of the measured normalized $t\bar{t}$ differential cross sections with different model predictions at the parton level for each of the kinematic variables.

	Approx. NNLO [62]		Approx. N^{3}LO [63]		NLO+NNLL' [65]		NNLO [66]	
Variable	χ^2/dof	p-value	χ^2/dof	p-value	χ^2/dof	p-value	χ^2/dof	p-value
p_T^t	27.9/5	<0.01	43.8/5	<0.01	24.1/5	<0.01	44.8/5	<0.01
y^t	4.2/7	0.76	3.75/7	0.81			3.8/7	0.80
$p_T^{t\bar{t}}$							4.0/4	0.40
$y^{t\bar{t}}$							7.6/7	0.37
$M^{t\bar{t}}$					68.3/5	<0.01	47.6/5	<0.01

Table 6. The χ^2/dof and p-values for the comparison of the measured normalized $t\bar{t}$ differential cross sections with published perturbative QCD calculations.

JHEP04(2018)060

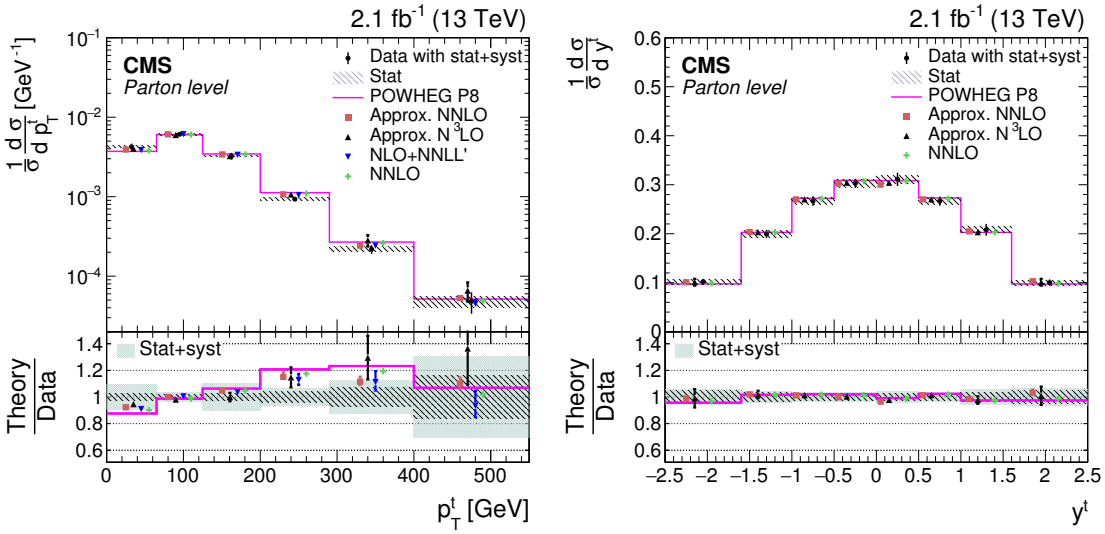

Figure 7. Normalized differential $t\bar{t}$ cross sections as a function of top quark p_T (left) and top quark rapidity (right), measured at the parton level in the full phase space and combining the distributions for top quarks and antiquarks. The vertical bars on the data points indicate the total (combined statistical and systematic) uncertainties, while the hatched band shows the statistical uncertainty. The measurements are compared to different perturbative QCD calculations of an approximate NNLO [62], an approximate next-to-NNLO (N^3LO) [63], an improved NLO+NNLL (NLO+NNLL') [65], and a full NNLO [66]. The lower panel gives the ratio of the theoretical predictions to the data.

JHEP04(2018)060

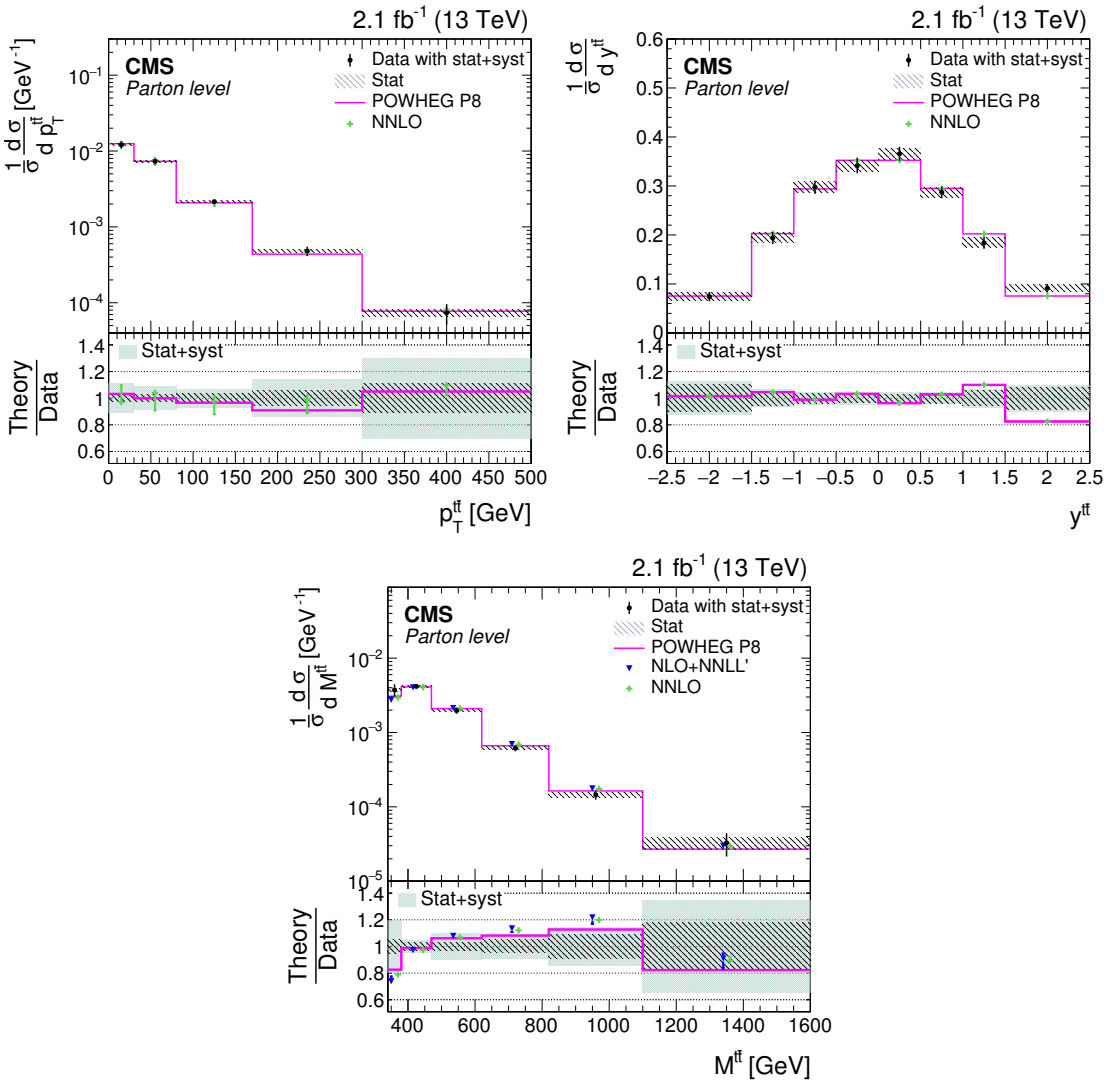

Figure 8. Normalized differential $\mathrm{t\bar{t}}$ cross sections as a function of $p_{\mathrm{T}}^{\mathrm{t\bar{t}}}$ (upper left), $y^{\mathrm{t\bar{t}}}$ (upper right), and $M^{\mathrm{t\bar{t}}}$ (lower) for the top quarks or antiquarks, measured at parton level in the full phase space. The vertical bars on the data points indicate the total (combined statistical and systematic) uncertainties, while the hatched band shows the statistical uncertainty. The measurements are compared to different perturbative QCD calculations of an improved NLO+NNLL (NLO+NNLL') [65] and a full NNLO [66]. The lower panel gives the ratio of the theoretical predictions to the data.

JHEP04(2018)060

Acknowledgments

We congratulate our colleagues in the CERN accelerator departments for the excellent performance of the LHC and thank the technical and administrative staffs at CERN and at other CMS institutes for their contributions to the success of the CMS effort. In addition, we gratefully acknowledge the computing centres and personnel of the Worldwide LHC Computing Grid for delivering so effectively the computing infrastructure essential to our analyses. Finally, we acknowledge the enduring support for the construction and operation of the LHC and the CMS detector provided by the following funding agencies: the Austrian Federal Ministry of Science, Research and Economy and the Austrian Science Fund; the Belgian Fonds de la Recherche Scientifique, and Fonds voor Wetenschappelijk Onderzoek; the Brazilian Funding Agencies (CNPq, CAPES, FAPERJ, and FAPESP); the Bulgarian Ministry of Education and Science; CERN; the Chinese Academy of Sciences, Ministry of Science and Technology, and National Natural Science Foundation of China; the Colombian Funding Agency (COLCIENCIAS); the Croatian Ministry of Science, Education and Sport, and the Croatian Science Foundation; the Research Promotion Foundation, Cyprus; the Secretariat for Higher Education, Science, Technology and Innovation, Ecuador; the Ministry of Education and Research, Estonian Research Council via IUT23-4 and IUT23-6 and European Regional Development Fund, Estonia; the Academy of Finland, Finnish Ministry of Education and Culture, and Helsinki Institute of Physics; the Institut National de Physique Nucléaire et de Physique des Particules / CNRS, and Commissariat à l'Énergie Atomique et aux Énergies Alternatives / CEA, France; the Bundesministerium für Bildung und Forschung, Deutsche Forschungsgemeinschaft, and Helmholtz-Gemeinschaft Deutscher Forschungszentren, Germany; the General Secretariat for Research and Technology, Greece; the National Scientific Research Foundation, and National Innovation Office, Hungary; the Department of Atomic Energy and the Department of Science and Technology, India; the Institute for Studies in Theoretical Physics and Mathematics, Iran; the Science Foundation, Ireland; the Istituto Nazionale di Fisica Nucleare, Italy; the Ministry of Science, ICT and Future Planning, and National Research Foundation (NRF), Republic of Korea; the Lithuanian Academy of Sciences; the Ministry of Education, and University of Malaya (Malaysia); the Mexican Funding Agencies (BUAP, CINVESTAV, CONACYT, LNS, SEP, and UASLP-FAI); the Ministry of Business, Innovation and Employment, New Zealand; the Pakistan Atomic Energy Commission; the Ministry of Science and Higher Education and the National Science Centre, Poland; the Fundação para a Ciência e a Tecnologia, Portugal; JINR, Dubna; the Ministry of Education and Science of the Russian Federation, the Federal Agency of Atomic Energy of the Russian Federation, Russian Academy of Sciences, the Russian Foundation for Basic Research and the Russian Competitiveness Program of NRNU "MEPhI"; the Ministry of Education, Science and Technological Development of Serbia; the Secretaría de Estado de Investigación, Desarrollo e Innovación, Programa Consolider-Ingenio 2010, Plan de Ciencia, Tecnología e Innovación 2013-2017 del Principado de Asturias and Fondo Europeo de Desarrollo Regional, Spain; the Swiss Funding Agencies (ETH Board, ETH Zurich, PSI, SNF, UniZH, Canton Zurich, and SER); the Ministry of Science and Technology, Taipei; the Thailand Center of Excellence in Physics,

JHEP04(2018)060

the Institute for the Promotion of Teaching Science and Technology of Thailand, Special Task Force for Activating Research and the National Science and Technology Development Agency of Thailand; the Scientific and Technical Research Council of Turkey, and Turkish Atomic Energy Authority; the National Academy of Sciences of Ukraine, and State Fund for Fundamental Researches, Ukraine; the Science and Technology Facilities Council, U.K.; the US Department of Energy, and the US National Science Foundation.

Individuals have received support from the Marie-Curie program and the European Research Council and Horizon 2020 Grant, contract No. 675440 (European Union); the Leventis Foundation; the A. P. Sloan Foundation; the Alexander von Humboldt Foundation; the Belgian Federal Science Policy Office; the Fonds pour la Formation à la Recherche dans l'Industrie et dans l'Agriculture (FRIA-Belgium); the Agentschap voor Innovatie door Wetenschap en Technologie (IWT-Belgium); the Ministry of Education, Youth and Sports (MEYS) of the Czech Republic; the Council of Scientific and Industrial Research, India; the HOMING PLUS program of the Foundation for Polish Science, cofinanced from European Union, Regional Development Fund, the Mobility Plus program of the Ministry of Science and Higher Education, the National Science Center (Poland), contracts Harmonia 2014/14/M/ST2/00428, Opus 2014/13/B/ST2/02543, 2014/15/B/ST2/03998, and 2015/19/B/ST2/02861, Sonata-bis 2012/07/E/ST2/01406; the National Priorities Research Program by Qatar National Research Fund; the Programa Clarín-COFUND del Principado de Asturias; the Thalis and Aristeia programs cofinanced by EU-ESF and the Greek NSRF; the Rachadapisek Sompot Fund for Postdoctoral Fellowship, Chulalongkorn University and the Chulalongkorn Academic into Its 2nd Century Project Advancement Project (Thailand); and the Welch Foundation, contract C-1845.

JHEP04(2018)060

A Tables of differential $\mathrm{t\bar{t}}$ cross sections at the particle level

$p_{\mathrm{T}}^{\mathrm{lep}}$ [GeV]	$(1/\sigma)(\mathrm{d}\sigma/\mathrm{d}p_{\mathrm{T}}^{\mathrm{lep}})$	stat	syst	factor
$[20, 30]$	2.00	0.04	0.03	$\times 10^{-2}$
$[30, 40]$	1.84	0.04	0.03	$\times 10^{-2}$
$[40, 60]$	1.38	0.02	0.01	$\times 10^{-2}$
$[60, 80]$	8.12	0.17	0.11	$\times 10^{-3}$
$[80, 120]$	3.12	0.07	0.09	$\times 10^{-3}$
$[120, 180]$	6.79	0.29	0.25	$\times 10^{-4}$
$[180, 400]$	5.01	0.44	0.33	$\times 10^{-5}$

Table 7. Normalized differential $\mathrm{t\bar{t}}$ cross sections with statistical and systematic uncertainties at the particle level as a function of $p_{\mathrm{T}}^{\mathrm{lep}}$. The factor given in the last column applies to the values of the normalized cross section and the statistical and systematic uncertainties in that row.

$p_{\mathrm{T}}^{\mathrm{jet}}$ [GeV]	$(1/\sigma)(\mathrm{d}\sigma/\mathrm{d}p_{\mathrm{T}}^{\mathrm{jet}})$	stat	syst	factor
$[30, 50]$	1.42	0.03	0.07	$\times 10^{-2}$
$[50, 80]$	1.12	0.02	0.02	$\times 10^{-2}$
$[80, 130]$	5.24	0.11	0.18	$\times 10^{-3}$
$[130, 210]$	1.18	0.04	0.06	$\times 10^{-3}$
$[210, 500]$	8.2	0.71	2.1	$\times 10^{-5}$

Table 8. Normalized differential $\mathrm{t\bar{t}}$ cross sections with statistical and systematic uncertainties at the particle level as a function of $p_{\mathrm{T}}^{\mathrm{jet}}$. The factor given in the last column applies to the values of the normalized cross section and the statistical and systematic uncertainties in that row.

$p_{\mathrm{T}}^{\mathrm{t}}$ [GeV]	$(1/\sigma)(\mathrm{d}\sigma/\mathrm{d}p_{\mathrm{T}}^{\mathrm{t}})$	stat	syst	factor
$[0, 65]$	4.14	0.12	0.13	$\times 10^{-3}$
$[65, 125]$	5.73	0.16	0.23	$\times 10^{-3}$
$[125, 200]$	3.20	0.10	0.13	$\times 10^{-3}$
$[200, 290]$	1.08	0.05	0.09	$\times 10^{-3}$
$[290, 400]$	3.42	0.27	0.54	$\times 10^{-4}$
$[400, 550]$	7.9	1.5	2.6	$\times 10^{-5}$

Table 9. Normalized differential $\mathrm{t\bar{t}}$ cross sections with statistical and systematic uncertainties at the particle level as a function of $p_{\mathrm{T}}^{\mathrm{t}}$. The factor given in the last column applies to the values of the normalized cross section and the statistical and systematic uncertainties in that row.

y^{t}	$(1/\sigma)(\mathrm{d}\sigma/\mathrm{d}y^{\mathrm{t}})$	stat	syst	factor
$[-2.5, -1.6]$	5.80	0.34	0.23	$\times 10^{-2}$
$[-1.6, -1.0]$	2.02	0.08	0.08	$\times 10^{-1}$
$[-1.0, -0.5]$	2.95	0.10	0.07	$\times 10^{-1}$
$[-0.5, 0.0]$	3.45	0.11	0.05	$\times 10^{-1}$
$[0.0, 0.5]$	3.57	0.11	0.11	$\times 10^{-1}$
$[0.5, 1.0]$	2.98	0.10	0.05	$\times 10^{-1}$
$[1.0, 1.6]$	2.12	0.08	0.08	$\times 10^{-1}$
$[1.6, 2.5]$	5.71	0.34	0.26	$\times 10^{-2}$

Table 10. Normalized differential $\mathrm{t\bar{t}}$ cross sections with statistical and systematic uncertainties at the particle level as a function of y^{t}. The factor given in the last column applies to the values of the normalized cross section and the statistical and systematic uncertainties in that row.

JHEP04(2018)060

$p_{\mathrm{T}}^{\mathrm{t\bar{t}}}$ [GeV]	$(1/\sigma)(\mathrm{d}\sigma/\mathrm{d}p_{\mathrm{T}}^{\mathrm{t\bar{t}}})$	stat	syst	factor
$[0, 30]$	1.01	0.03	0.14	$\times 10^{-2}$
$[30, 80]$	8.16	0.26	0.65	$\times 10^{-3}$
$[80, 170]$	2.34	0.10	0.17	$\times 10^{-3}$
$[170, 300]$	4.81	0.39	0.72	$\times 10^{-4}$
$[300, 500]$	7.6	1.3	2.6	$\times 10^{-5}$

Table 11. Normalized differential $\mathrm{t\bar{t}}$ cross sections with statistical and systematic uncertainties at the particle level as a function of $p_{\mathrm{T}}^{\mathrm{t\bar{t}}}$. The factor given in the last column applies to the values of the normalized cross section and the statistical and systematic uncertainties in that row.

$y^{\mathrm{t\bar{t}}}$	$(1/\sigma)(\mathrm{d}\sigma/\mathrm{d}y^{\mathrm{t\bar{t}}})$	stat	syst	factor
$[-2.5, -1.5]$	2.57	0.32	0.19	$\times 10^{-2}$
$[-1.5, -1.0]$	1.68	0.10	0.07	$\times 10^{-1}$
$[-1.0, -0.5]$	3.37	0.14	0.04	$\times 10^{-1}$
$[-0.5, 0.0]$	4.30	0.16	0.11	$\times 10^{-1}$
$[0.0, 0.5]$	4.60	0.16	0.06	$\times 10^{-1}$
$[0.5, 1.0]$	3.28	0.14	0.08	$\times 10^{-1}$
$[1.0, 1.5]$	1.58	0.10	0.07	$\times 10^{-1}$
$[1.5, 2.5]$	3.35	0.33	0.20	$\times 10^{-2}$

Table 12. Normalized differential $\mathrm{t\bar{t}}$ cross sections with statistical and systematic uncertainties at the particle level as a function of $y^{\mathrm{t\bar{t}}}$. The factor given in the last column applies to the values of the normalized cross section and the statistical and systematic uncertainties in that row.

$M^{\mathrm{t\bar{t}}}$ [GeV]	$(1/\sigma)(\mathrm{d}\sigma/\mathrm{d}M^{\mathrm{t\bar{t}}})$	stat	syst	factor
$[300, 400]$	3.07	0.13	0.12	$\times 10^{-3}$
$[400, 500]$	3.07	0.15	0.20	$\times 10^{-3}$
$[500, 650]$	1.44	0.08	0.08	$\times 10^{-3}$
$[650, 1000]$	3.85	0.26	0.80	$\times 10^{-4}$
$[1000, 1600]$	5.9	0.90	1.6	$\times 10^{-5}$

Table 13. Normalized differential $\mathrm{t\bar{t}}$ cross sections with statistical and systematic uncertainties at the particle level as a function of $M^{\mathrm{t\bar{t}}}$. The factor given in the last column applies to the values of the normalized cross section and the statistical and systematic uncertainties in that row.

JHEP04(2018)060

$\Delta\phi^{t\bar{t}}$ [rad]	$(1/\sigma)(d\sigma/d\Delta\phi^{t\bar{t}})$	stat	syst	factor
$[0, 1.57]$	6.79	0.60	1.04	$\times 10^{-2}$
$[1.57, 2.61]$	2.26	0.14	0.26	$\times 10^{-1}$
$[2.61, 3.016]$	9.52	0.44	0.71	$\times 10^{-1}$
$[3.016, 3.142]$	2.2	0.10	0.41	$\times 1$

Table 14. Normalized differential $t\bar{t}$ cross sections with statistical and systematic uncertainties at the particle level as a function of $\Delta\phi^{t\bar{t}}$. The factor given in the last column applies to the values of the normalized cross section and the statistical and systematic uncertainties in that row.

B Tables of differential cross section at the parton level

p_T^t [GeV]	$(1/\sigma)(d\sigma/dp_T^t)$	stat	syst	factor
$[0, 65]$	4.24	0.11	0.40	$\times 10^{-3}$
$[65, 125]$	6.10	0.13	0.14	$\times 10^{-3}$
$[125, 200]$	3.25	0.08	0.31	$\times 10^{-3}$
$[200, 290]$	9.31	0.37	0.47	$\times 10^{-4}$
$[290, 400]$	2.18	0.16	0.22	$\times 10^{-4}$
$[400, 550]$	4.8	0.79	1.2	$\times 10^{-5}$

Table 15. Normalized differential $t\bar{t}$ cross sections with statistical and systematic uncertainties at the parton level as a function of p_T^t. The factor given in the last column applies to the values of the normalized cross section and the statistical and systematic uncertainties in that row.

y^t	$(1/\sigma)(d\sigma/dy^t)$	stat	syst	factor
$[-2.5, -1.6]$	1.02	0.05	0.03	$\times 10^{-1}$
$[-1.6, -1.0]$	1.99	0.06	0.05	$\times 10^{-1}$
$[-1.0, -0.5]$	2.67	0.08	0.06	$\times 10^{-1}$
$[-0.5, 0.0]$	3.03	0.08	0.04	$\times 10^{-1}$
$[0.0, 0.5]$	3.11	0.08	0.11	$\times 10^{-1}$
$[0.5, 1.0]$	2.67	0.08	0.05	$\times 10^{-1}$
$[1.0, 1.6]$	2.08	0.06	0.10	$\times 10^{-1}$
$[1.6, 2.5]$	1.00	0.05	0.05	$\times 10^{-1}$

Table 16. Normalized differential $t\bar{t}$ cross sections with statistical and systematic uncertainties at the parton level as a function of y^t. The factor given in the last column applies to the values of the normalized cross section and the statistical and systematic uncertainties in that row.

JHEP04(2018)060

$p_{\mathrm{T}}^{\mathrm{t\bar{t}}}$ [GeV]	$(1/\sigma)(\mathrm{d}\sigma/\mathrm{d}p_{\mathrm{T}}^{\mathrm{t\bar{t}}})$	stat	syst	factor
$[0, 30]$	1.21	0.03	0.13	$\times 10^{-2}$
$[30, 80]$	7.32	0.18	0.61	$\times 10^{-3}$
$[80, 170]$	2.15	0.07	0.13	$\times 10^{-3}$
$[170, 300]$	4.81	0.27	0.62	$\times 10^{-4}$
$[300, 500]$	7.4	0.79	2.1	$\times 10^{-5}$

Table 17. Normalized differential $\mathrm{t\bar{t}}$ cross sections with statistical and systematic uncertainties at the parton level as a function of $p_{\mathrm{T}}^{\mathrm{t\bar{t}}}$. The factor given in the last column applies to the values of the normalized cross section and the statistical and systematic uncertainties in that row.

$y^{\mathrm{t\bar{t}}}$	$(1/\sigma)(\mathrm{d}\sigma/\mathrm{d}y^{\mathrm{t\bar{t}}})$	stat	syst	factor
$[-2.5, -1.5]$	7.42	0.75	0.54	$\times 10^{-2}$
$[-1.5, -1.0]$	1.94	0.10	0.07	$\times 10^{-1}$
$[-1.0, -0.5]$	2.97	0.11	0.08	$\times 10^{-1}$
$[-0.5, 0.0]$	3.41	0.11	0.10	$\times 10^{-1}$
$[0.0, 0.5]$	3.66	0.11	0.09	$\times 10^{-1}$
$[0.5, 1.0]$	2.87	0.11	0.05	$\times 10^{-1}$
$[1.0, 1.5]$	1.84	0.10	0.07	$\times 10^{-1}$
$[1.5, 2.5]$	9.14	0.76	0.45	$\times 10^{-2}$

Table 18. Normalized differential $\mathrm{t\bar{t}}$ cross sections with statistical and systematic uncertainties at the parton level as a function of $y^{\mathrm{t\bar{t}}}$. The factor given in the last column applies to the values of the normalized cross section and the statistical and systematic uncertainties in that row.

$M^{\mathrm{t\bar{t}}}$ [GeV]	$(1/\sigma)(\mathrm{d}\sigma/\mathrm{d}M^{\mathrm{t\bar{t}}})$	stat	syst	factor
$[340, 380]$	3.73	0.20	0.70	$\times 10^{-3}$
$[380, 470]$	4.16	0.11	0.15	$\times 10^{-3}$
$[470, 620]$	1.97	0.06	0.18	$\times 10^{-3}$
$[620, 820]$	6.14	0.30	0.48	$\times 10^{-4}$
$[820, 1100]$	1.45	0.13	0.15	$\times 10^{-4}$
$[1100, 1600]$	3.28	0.59	0.97	$\times 10^{-5}$

Table 19. Normalized differential $\mathrm{t\bar{t}}$ cross sections with statistical and systematic uncertainties at the parton level as a function of $M^{\mathrm{t\bar{t}}}$. The factor given in the last column applies to the values of the normalized cross section and the statistical and systematic uncertainties in that row.

JHEP04(2018)060

$\Delta\phi^{t\bar{t}}$ [rad]	$(1/\sigma)(d\sigma/d\Delta\phi^{t\bar{t}})$	stat	syst	factor
$[0, 1.57]$	7.02	0.48	0.92	$\times 10^{-2}$
$[1.57, 2.61]$	2.14	0.11	0.24	$\times 10^{-1}$
$[2.61, 3.016]$	9.30	0.37	0.53	$\times 10^{-1}$
$[3.016, 3.142]$	2.30	0.09	0.33	$\times 1$

Table 20. Normalized differential $t\bar{t}$ cross sections with statistical and systematic uncertainties at the parton level as a function of $\Delta\phi^{t\bar{t}}$. The factor given in the last column applies to the values of the normalized cross section and the statistical and systematic uncertainties in that row.

References

[1] M. Czakon, M.L. Mangano, A. Mitov and J. Rojo, *Constraints on the gluon PDF from top quark pair production at hadron colliders*, *JHEP* **07** (2013) 167 [arXiv:1303.7215] [INSPIRE].

[2] CMS collaboration, *Measurement of differential top-quark pair production cross sections in pp colisions at $\sqrt{s} = 7$ TeV*, *Eur. Phys. J.* **C 73** (2013) 2339 [arXiv:1211.2220] [INSPIRE].

[3] ATLAS collaboration, *Differential top-antitop cross-section measurements as a function of observables constructed from final-state particles using pp collisions at $\sqrt{s} = 7$ TeV in the ATLAS detector*, *JHEP* **06** (2015) 100 [arXiv:1502.05923] [INSPIRE].

[4] CMS collaboration, *Measurement of the differential cross section for top quark pair production in pp collisions at $\sqrt{s} = 8$ TeV*, *Eur. Phys. J.* **C 75** (2015) 542 [arXiv:1505.04480] [INSPIRE].

[5] ATLAS collaboration, *Measurements of top-quark pair differential cross-sections in the lepton+jets channel in pp collisions at $\sqrt{s} = 8$ TeV using the ATLAS detector*, *Eur. Phys. J.* **C 76** (2016) 538 [arXiv:1511.04716] [INSPIRE].

[6] CMS collaboration, *Measurement of the differential cross sections for top quark pair production as a function of kinematic event variables in pp collisions at $\sqrt{s} = 7$ and 8 TeV*, *Phys. Rev.* **D 94** (2016) 052006 [arXiv:1607.00837] [INSPIRE].

[7] CMS collaboration, *Measurement of the integrated and differential $t\bar{t}$ production cross sections for high-p_t top quarks in pp collisions at $\sqrt{s} = 8$ TeV*, *Phys. Rev.* **D 94** (2016) 072002 [arXiv:1605.00116] [INSPIRE].

[8] CMS collaboration, *Measurement of the $t\bar{t}$ production cross section in the all-jets final state in pp collisions at $\sqrt{s} = 8$ TeV*, *Eur. Phys. J.* **C 76** (2016) 128 [arXiv:1509.06076] [INSPIRE].

[9] CMS collaboration, *Measurement of $t\bar{t}$ production with additional jet activity, including b quark jets, in the dilepton decay channel using pp collisions at $\sqrt{s} = 8$ TeV*, *Eur. Phys. J.* **C 76** (2016) 379 [arXiv:1510.03072] [INSPIRE].

[10] ATLAS collaboration, *Measurement of jet activity in top quark events using the $e\mu$ final state with two b-tagged jets in pp collisions at $\sqrt{s} = 8$ TeV with the ATLAS detector*, *JHEP* **09** (2016) 074 [arXiv:1606.09490] [INSPIRE].

JHEP04(2018)060

[11] ATLAS collaboration, *Measurement of top quark pair differential cross-sections in the dilepton channel in pp collisions at $\sqrt{s} = 7$ and 8 TeV with ATLAS*, *Phys. Rev.* **D 94** (2016) 092003 [arXiv:1607.07281] [INSPIRE].

[12] CMS collaboration, *Measurement of double-differential cross sections for top quark pair production in pp collisions at $\sqrt{s} = 8$ TeV and impact on parton distribution functions*, *Eur. Phys. J.* **C 77** (2017) 459 [arXiv:1703.01630] [INSPIRE].

[13] CMS collaboration, *Measurement of differential cross sections for top quark pair production using the lepton+jets final state in proton-proton collisions at 13 TeV*, *Phys. Rev.* **D 95** (2017) 092001 [arXiv:1610.04191] [INSPIRE].

[14] ATLAS collaboration, *Measurement of jet activity produced in top-quark events with an electron, a muon and two b-tagged jets in the final state in pp collisions at $\sqrt{s} = 13$ TeV with the ATLAS detector*, *Eur. Phys. J.* **C 77** (2017) 220 [arXiv:1610.09978] [INSPIRE].

[15] ATLAS collaboration, *Measurements of top-quark pair differential cross-sections in the eμ channel in pp collisions at $\sqrt{s} = 13$ TeV using the ATLAS detector*, *Eur. Phys. J.* **C 77** (2017) 292 [arXiv:1612.05220] [INSPIRE].

[16] S. Choi and H.S. Lee, *Azimuthal decorrelation in $t\bar{t}$ production at hadron colliders*, *Phys. Rev.* **D 87** (2013) 034012 [arXiv:1207.1484] [INSPIRE].

[17] CMS collaboration, *The CMS experiment at the CERN LHC*, 2008 *JINST* **3** S08004 [INSPIRE].

[18] CMS collaboration, *Particle-flow reconstruction and global event description with the CMS detector*, 2017 *JINST* **12** P10003 [arXiv:1706.04965] [INSPIRE].

[19] CMS collaboration, *Missing transverse energy performance of the CMS detector*, 2011 *JINST* **6** P09001 [arXiv:1106.5048] [INSPIRE].

[20] P. Nason, *A New method for combining NLO QCD with shower Monte Carlo algorithms*, *JHEP* **11** (2004) 040 [hep-ph/0409146] [INSPIRE].

[21] S. Frixione, P. Nason and C. Oleari, *Matching NLO QCD computations with parton shower simulations: the POWHEG method*, *JHEP* **11** (2007) 070 [arXiv:0709.2092] [INSPIRE].

[22] S. Alioli, P. Nason, C. Oleari and E. Re, *A general framework for implementing NLO calculations in shower Monte Carlo programs: the POWHEG BOX*, *JHEP* **06** (2010) 043 [arXiv:1002.2581] [INSPIRE].

[23] J.M. Campbell, R.K. Ellis, P. Nason and E. Re, *Top-Pair Production and Decay at NLO Matched with Parton Showers*, *JHEP* **04** (2015) 114 [arXiv:1412.1828] [INSPIRE].

[24] J. Alwall et al., *The automated computation of tree-level and next-to-leading order differential cross sections and their matching to parton shower simulations*, *JHEP* **07** (2014) 079 [arXiv:1405.0301] [INSPIRE].

[25] T. Sjöstrand, S. Mrenna and P.Z. Skands, *A brief introduction to PYTHIA 8.1*, *Comput. Phys. Commun.* **178** (2008) 852 [arXiv:0710.3820] [INSPIRE].

[26] P. Skands, S. Carrazza and J. Rojo, *Tuning PYTHIA 8.1: the Monash 2013 Tune*, *Eur. Phys. J.* **C 74** (2014) 3024 [arXiv:1404.5630] [INSPIRE].

[27] R. Frederix and S. Frixione, *Merging meets matching in MC@NLO*, *JHEP* **12** (2012) 061 [arXiv:1209.6215] [INSPIRE].

[28] J. Alwall et al., *Comparative study of various algorithms for the merging of parton showers and matrix elements in hadronic collisions*, *Eur. Phys. J.* **C 53** (2008) 473 [arXiv:0706.2569] [INSPIRE].

JHEP04(2018)060

[29] M. Bahr et al., *HERWIG++ physics and manual*, *Eur. Phys. J.* **C 58** (2008) 639 [arXiv:0803.0883] [INSPIRE].

[30] M.H. Seymour and A. Siodmok, *Constraining MPI models using $\sigma_{\rm eff}$ and recent Tevatron and LHC Underlying Event data*, *JHEP* **10** (2013) 113 [arXiv:1307.5015] [INSPIRE].

[31] M. Czakon and A. Mitov, *Top++: A program for the calculation of the top-pair cross-section at hadron colliders*, *Comput. Phys. Commun.* **185** (2014) 2930 [arXiv:1112.5675] [INSPIRE].

[32] Y. Li and F. Petriello, *Combining QCD and electroweak corrections to dilepton production in FEWZ*, *Phys. Rev.* **D 86** (2012) 094034 [arXiv:1208.5967] [INSPIRE].

[33] S. Frixione, E. Laenen, P. Motylinski, B.R. Webber and C.D. White, *Single-top hadroproduction in association with a W boson*, *JHEP* **07** (2008) 029 [arXiv:0805.3067] [INSPIRE].

[34] E. Re, *Single-top Wt-channel production matched with parton showers using the POWHEG method*, *Eur. Phys. J.* **C 71** (2011) 1547 [arXiv:1009.2450] [INSPIRE].

[35] N. Kidonakis, *NNLL threshold resummation for top-pair and single-top production*, *Phys. Part. Nucl.* **45** (2014) 714 [arXiv:1210.7813] [INSPIRE].

[36] T. Gehrmann et al., *W^+W^- production at hadron colliders in next to next to leading order QCD*, *Phys. Rev. Lett.* **113** (2014) 212001 [arXiv:1408.5243] [INSPIRE].

[37] J.M. Campbell and R.K. Ellis, *MCFM for the Tevatron and the LHC*, *Nucl. Phys. Proc. Suppl.* **205-206** (2010) 10 [arXiv:1007.3492] [INSPIRE].

[38] J. Allison et al., *GEANT4 developments and applications*, *IEEE Trans. Nucl. Sci.* **53** (2006) 270.

[39] GEANT4 collaboration, S. Agostinelli et al., *GEANT4 — a simulation toolkit*, *Nucl. Instrum. Meth.* **A 506** (2003) 250 [INSPIRE].

[40] CMS collaboration, *Measurement of the $\mathrm{t\bar{t}}$ production cross section using events in the $\mathrm{e}\mu$ final state in pp collisions at $\sqrt{s} = 13$ TeV*, *Eur. Phys. J.* **C 77** (2017) 172 [arXiv:1611.04040] [INSPIRE].

[41] CMS collaboration, *Performance of CMS muon reconstruction in pp collision events at $\sqrt{s} = 7$ TeV*, 2012 *JINST* **7** P10002 [arXiv:1206.4071] [INSPIRE].

[42] CMS collaboration, *Performance of Electron Reconstruction and Selection with the CMS Detector in Proton-Proton Collisions at $\sqrt{s} = 8$ TeV*, 2015 *JINST* **10** P06005 [arXiv:1502.02701] [INSPIRE].

[43] CMS collaboration, *Measurement of the top quark pair production cross section in proton-proton collisions at $\sqrt{s} = 13$ TeV*, *Phys. Rev. Lett.* **116** (2016) 052002 [arXiv:1510.05302] [INSPIRE].

[44] M. Cacciari, G.P. Salam and G. Soyez, *FastJet user manual*, *Eur. Phys. J.* **C 72** (2012) 1896 [arXiv:1111.6097] [INSPIRE].

[45] M. Cacciari, G.P. Salam and G. Soyez, *The anti-k_t jet clustering algorithm*, *JHEP* **04** (2008) 063 [arXiv:0802.1189] [INSPIRE].

[46] CMS collaboration, *Jet energy scale and resolution in the CMS experiment in pp collisions at 8 TeV*, 2017 *JINST* **12** P02014 [arXiv:1607.03663] [INSPIRE].

[47] CMS collaboration, *Identification of b-quark jets with the CMS experiment*, 2013 *JINST* **8** P04013 [arXiv:1211.4462] [INSPIRE].

JHEP04(2018)060

[48] CMS collaboration, *Identification of b quark jets at the CMS Experiment in the LHC Run 2*, CMS-PAS-BTV-15-001 (2016).

[49] Particle Data Group collaboration, C. Patrignani et al., *Review of particle physics*, *Chin. Phys.* **C 40** (2016) 100001 [INSPIRE].

[50] L. Sonnenschein, *Analytical solution of $t\bar{t}$ dilepton equations*, *Phys. Rev.* **D 73** (2006) 054015 [*Erratum ibid.* **D 78** (2008) 079902] [hep-ph/0603011] [INSPIRE].

[51] R.H. Dalitz and G.R. Goldstein, *Analysis of top-antitop production and dilepton decay events and the top quark mass*, *Phys. Lett.* **B 287** (1992) 225 [INSPIRE].

[52] CMS collaboration, *First measurement of the cross section for top-quark pair production in proton-proton collisions at $\sqrt{s} = 7$ TeV*, *Phys. Lett.* **B 695** (2011) 424 [arXiv:1010.5994] [INSPIRE].

[53] CMS collaboration, *Measurement of the $\mathrm{t\bar{t}}$ production cross section and the top quark mass in the dilepton channel in pp collisions at $\sqrt{s} = 7$ TeV*, *JHEP* **07** (2011) 049 [arXiv:1105.5661] [INSPIRE].

[54] CMS collaboration, *Measurement of the $\mathrm{t\bar{t}}$ production cross section in the dilepton channel in pp collisions at $\sqrt{s} = 7$ TeV*, *JHEP* **11** (2012) 067 [arXiv:1208.2671] [INSPIRE].

[55] G. D'Agostini, *A multidimensional unfolding method based on Bayes' theorem*, *Nucl. Instrum. Meth.* **A 362** (1995) 487 [INSPIRE].

[56] CMS collaboration, *Determination of jet energy calibration and transverse momentum resolution in CMS*, 2011 *JINST* **6** P11002 [arXiv:1107.4277] [INSPIRE].

[57] NNPDF collaboration, R.D. Ball et al., *Parton distributions for the LHC Run II*, *JHEP* **04** (2015) 040 [arXiv:1410.8849] [INSPIRE].

[58] J. Butterworth et al., *PDF4LHC recommendations for LHC Run II*, *J. Phys.* **G 43** (2016) 023001 [arXiv:1510.03865] [INSPIRE].

[59] M. Cacciari, S. Frixione, M.L. Mangano, P. Nason and G. Ridolfi, *The $t\bar{t}$ cross-section at 1.8 TeV and 1.96 TeV: A study of the systematics due to parton densities and scale dependence*, *JHEP* **04** (2004) 068 [hep-ph/0303085] [INSPIRE].

[60] S. Catani, D. de Florian, M. Grazzini and P. Nason, *Soft gluon resummation for Higgs boson production at hadron colliders*, *JHEP* **07** (2003) 028 [hep-ph/0306211] [INSPIRE].

[61] E. Gross and O. Vitells, *Trial factors for the look elsewhere effect in high energy physics*, *Eur. Phys. J.* **C 70** (2010) 525 [arXiv:1005.1891] [INSPIRE].

[62] M. Guzzi, K. Lipka and S.-O. Moch, *Top-quark pair production at hadron colliders: differential cross section and phenomenological applications with DiffTop*, *JHEP* **01** (2015) 082 [arXiv:1406.0386] [INSPIRE].

[63] N. Kidonakis, *NNNLO soft-gluon corrections for the top-quark p_{T} and rapidity distributions*, *Phys. Rev.* **D 91** (2015) 031501 [arXiv:1411.2633] [INSPIRE].

[64] L.A. Harland-Lang, A.D. Martin, P. Motylinski and R.S. Thorne, *Parton distributions in the LHC era: MMHT 2014 PDFs*, *Eur. Phys. J.* **C 75** (2015) 204 [arXiv:1412.3989] [INSPIRE].

[65] B.D. Pecjak, D.J. Scott, X. Wang and L.L. Yang, *Resummed differential cross sections for top-quark pairs at the LHC*, *Phys. Rev. Lett.* **116** (2016) 202001 [arXiv:1601.07020] [INSPIRE].

[66] M. Czakon, D. Heymes and A. Mitov, *High-precision differential predictions for top-quark pairs at the LHC*, *Phys. Rev. Lett.* **116** (2016) 082003 [arXiv:1511.00549] [INSPIRE].

JHEP04(2018)060

The CMS collaboration

Yerevan Physics Institute, Yerevan, Armenia

A.M. Sirunyan, A. Tumasyan

Institut für Hochenergiephysik, Wien, Austria

W. Adam, F. Ambrogi, E. Asilar, T. Bergauer, J. Brandstetter, E. Brondolin, M. Dragicevic, J. Erö, M. Flechl, M. Friedl, R. Frühwirth[1], V.M. Ghete, J. Grossmann, J. Hrubec, M. Jeitler[1], A. König, N. Krammer, I. Krätschmer, D. Liko, T. Madlener, I. Mikulec, E. Pree, D. Rabady, N. Rad, H. Rohringer, J. Schieck[1], R. Schöfbeck, M. Spanring, D. Spitzbart, J. Strauss, W. Waltenberger, J. Wittmann, C.-E. Wulz[1], M. Zarucki

Institute for Nuclear Problems, Minsk, Belarus

V. Chekhovsky, V. Mossolov, J. Suarez Gonzalez

Universiteit Antwerpen, Antwerpen, Belgium

E.A. De Wolf, X. Janssen, J. Lauwers, M. Van De Klundert, H. Van Haevermaet, P. Van Mechelen, N. Van Remortel, A. Van Spilbeeck

Vrije Universiteit Brussel, Brussel, Belgium

S. Abu Zeid, F. Blekman, J. D'Hondt, I. De Bruyn, J. De Clercq, K. Deroover, G. Flouris, S. Lowette, S. Moortgat, L. Moreels, A. Olbrechts, Q. Python, K. Skovpen, S. Tavernier, W. Van Doninck, P. Van Mulders, I. Van Parijs

Université Libre de Bruxelles, Bruxelles, Belgium

H. Brun, B. Clerbaux, G. De Lentdecker, H. Delannoy, G. Fasanella, L. Favart, R. Goldouzian, A. Grebenyuk, G. Karapostoli, T. Lenzi, J. Luetic, T. Maerschalk, A. Marinov, A. Randle-conde, T. Seva, C. Vander Velde, P. Vanlaer, D. Vannerom, R. Yonamine, F. Zenoni, F. Zhang[2]

Ghent University, Ghent, Belgium

A. Cimmino, T. Cornelis, D. Dobur, A. Fagot, M. Gul, I. Khvastunov, D. Poyraz, C. Roskas, S. Salva, M. Tytgat, W. Verbeke, N. Zaganidis

Université Catholique de Louvain, Louvain-la-Neuve, Belgium

H. Bakhshiansohi, O. Bondu, S. Brochet, G. Bruno, A. Caudron, S. De Visscher, C. Delaere, M. Delcourt, B. Francois, A. Giammanco, A. Jafari, M. Komm, G. Krintiras, V. Lemaitre, A. Magitteri, A. Mertens, M. Musich, K. Piotrzkowski, L. Quertenmont, M. Vidal Marono, S. Wertz

Université de Mons, Mons, Belgium

N. Beliy

Centro Brasileiro de Pesquisas Fisicas, Rio de Janeiro, Brazil

W.L. Aldá Júnior, F.L. Alves, G.A. Alves, L. Brito, M. Correa Martins Junior, C. Hensel, A. Moraes, M.E. Pol, P. Rebello Teles

JHEP04(2018)060

Universidade do Estado do Rio de Janeiro, Rio de Janeiro, Brazil

E. Belchior Batista Das Chagas, W. Carvalho, J. Chinellato[3], A. Custódio, E.M. Da Costa, G.G. Da Silveira[4], D. De Jesus Damiao, S. Fonseca De Souza, L.M. Huertas Guativa, H. Malbouisson, M. Melo De Almeida, C. Mora Herrera, L. Mundim, H. Nogima, A. Santoro, A. Sznajder, E.J. Tonelli Manganote[3], F. Torres Da Silva De Araujo, A. Vilela Pereira

Universidade Estadual Paulista [a], Universidade Federal do ABC [b], São Paulo, Brazil

S. Ahuja[a], C.A. Bernardes[a], T.R. Fernandez Perez Tomei[a], E.M. Gregores[b], P.G. Mercadante[b], C.S. Moon[a], S.F. Novaes[a], Sandra S. Padula[a], D. Romero Abad[b], J.C. Ruiz Vargas[a]

Institute for Nuclear Research and Nuclear Energy of Bulgaria Academy of Sciences

A. Aleksandrov, R. Hadjiiska, P. Iaydjiev, M. Misheva, M. Rodozov, S. Stoykova, G. Sultanov, M. Vutova

University of Sofia, Sofia, Bulgaria

A. Dimitrov, I. Glushkov, L. Litov, B. Pavlov, P. Petkov

Beihang University, Beijing, China

W. Fang[5], X. Gao[5]

Institute of High Energy Physics, Beijing, China

M. Ahmad, J.G. Bian, G.M. Chen, H.S. Chen, M. Chen, Y. Chen, C.H. Jiang, D. Leggat, Z. Liu, F. Romeo, S.M. Shaheen, A. Spiezia, J. Tao, C. Wang, Z. Wang, E. Yazgan, H. Zhang, J. Zhao

State Key Laboratory of Nuclear Physics and Technology, Peking University, Beijing, China

Y. Ban, G. Chen, Q. Li, S. Liu, Y. Mao, S.J. Qian, D. Wang, Z. Xu

Universidad de Los Andes, Bogota, Colombia

C. Avila, A. Cabrera, L.F. Chaparro Sierra, C. Florez, C.F. González Hernández, J.D. Ruiz Alvarez

University of Split, Faculty of Electrical Engineering, Mechanical Engineering and Naval Architecture, Split, Croatia

B. Courbon, N. Godinovic, D. Lelas, I. Puljak, P.M. Ribeiro Cipriano, T. Sculac

University of Split, Faculty of Science, Split, Croatia

Z. Antunovic, M. Kovac

Institute Rudjer Boskovic, Zagreb, Croatia

V. Brigljevic, D. Ferencek, K. Kadija, B. Mesic, T. Susa

JHEP04(2018)060

University of Cyprus, Nicosia, Cyprus

M.W. Ather, A. Attikis, G. Mavromanolakis, J. Mousa, C. Nicolaou, F. Ptochos, P.A. Razis, H. Rykaczewski

Charles University, Prague, Czech Republic

M. Finger[6], M. Finger Jr.[6]

Universidad San Francisco de Quito, Quito, Ecuador

E. Carrera Jarrin

Academy of Scientific Research and Technology of the Arab Republic of Egypt, Egyptian Network of High Energy Physics, Cairo, Egypt

A.A. Abdelalim[7,8], Y. Mohammed[9], E. Salama[10,11]

National Institute of Chemical Physics and Biophysics, Tallinn, Estonia

R.K. Dewanjee, M. Kadastik, L. Perrini, M. Raidal, A. Tiko, C. Veelken

Department of Physics, University of Helsinki, Helsinki, Finland

P. Eerola, J. Pekkanen, M. Voutilainen

Helsinki Institute of Physics, Helsinki, Finland

J. Härkönen, T. Järvinen, V. Karimäki, R. Kinnunen, T. Lampén, K. Lassila-Perini, S. Lehti, T. Lindén, P. Luukka, E. Tuominen, J. Tuominiemi, E. Tuovinen

Lappeenranta University of Technology, Lappeenranta, Finland

J. Talvitie, T. Tuuva

IRFU, CEA, Université Paris-Saclay, Gif-sur-Yvette, France

M. Besancon, F. Couderc, M. Dejardin, D. Denegri, J.L. Faure, F. Ferri, S. Ganjour, S. Ghosh, A. Givernaud, P. Gras, G. Hamel de Monchenault, P. Jarry, I. Kucher, E. Locci, M. Machet, J. Malcles, G. Negro, J. Rander, A. Rosowsky, M.Ö. Sahin, M. Titov

Laboratoire Leprince-Ringuet, Ecole polytechnique, CNRS/IN2P3, Université Paris-Saclay, Palaiseau, France

A. Abdulsalam, I. Antropov, S. Baffioni, F. Beaudette, P. Busson, L. Cadamuro, C. Charlot, O. Davignon, R. Granier de Cassagnac, M. Jo, S. Lisniak, A. Lobanov, J. Martin Blanco, M. Nguyen, C. Ochando, G. Ortona, P. Paganini, P. Pigard, S. Regnard, R. Salerno, J.B. Sauvan, Y. Sirois, A.G. Stahl Leiton, T. Strebler, Y. Yilmaz, A. Zabi, A. Zghiche

Université de Strasbourg, CNRS, IPHC UMR 7178, F-67000 Strasbourg, France

J.-L. Agram[12], J. Andrea, D. Bloch, J.-M. Brom, M. Buttignol, E.C. Chabert, N. Chanon, C. Collard, E. Conte[12], X. Coubez, J.-C. Fontaine[12], D. Gelé, U. Goerlach, M. Jansová, A.-C. Le Bihan, P. Van Hove

Centre de Calcul de l'Institut National de Physique Nucleaire et de Physique des Particules, CNRS/IN2P3, Villeurbanne, France

S. Gadrat

JHEP04(2018)060

Université de Lyon, Université Claude Bernard Lyon 1, CNRS-IN2P3, Institut de Physique Nucléaire de Lyon, Villeurbanne, France

S. Beauceron, C. Bernet, G. Boudoul, R. Chierici, D. Contardo, P. Depasse, H. El Mamouni, J. Fay, L. Finco, S. Gascon, M. Gouzevitch, G. Grenier, B. Ille, F. Lagarde, I.B. Laktineh, M. Lethuillier, L. Mirabito, A.L. Pequegnot, S. Perries, A. Popov[13], V. Sordini, M. Vander Donckt, S. Viret

Georgian Technical University, Tbilisi, Georgia

A. Khvedelidze[6]

Tbilisi State University, Tbilisi, Georgia

Z. Tsamalaidze[6]

RWTH Aachen University, I. Physikalisches Institut, Aachen, Germany

C. Autermann, S. Beranek, L. Feld, M.K. Kiesel, K. Klein, M. Lipinski, M. Preuten, C. Schomakers, J. Schulz, T. Verlage

RWTH Aachen University, III. Physikalisches Institut A, Aachen, Germany

A. Albert, M. Brodski, E. Dietz-Laursonn, D. Duchardt, M. Endres, M. Erdmann, S. Erdweg, T. Esch, R. Fischer, A. Güth, M. Hamer, T. Hebbeker, C. Heidemann, K. Hoepfner, S. Knutzen, M. Merschmeyer, A. Meyer, P. Millet, S. Mukherjee, M. Olschewski, K. Padeken, T. Pook, M. Radziej, H. Reithler, M. Rieger, F. Scheuch, D. Teyssier, S. Thüer

RWTH Aachen University, III. Physikalisches Institut B, Aachen, Germany

G. Flügge, B. Kargoll, T. Kress, A. Künsken, J. Lingemann, T. Müller, A. Nehrkorn, A. Nowack, C. Pistone, O. Pooth, A. Stahl[14]

Deutsches Elektronen-Synchrotron, Hamburg, Germany

M. Aldaya Martin, T. Arndt, C. Asawatangtrakuldee, K. Beernaert, O. Behnke, U. Behrens, A.A. Bin Anuar, K. Borras[15], V. Botta, A. Campbell, P. Connor, C. Contreras-Campana, F. Costanza, C. Diez Pardos, G. Eckerlin, D. Eckstein, T. Eichhorn, E. Eren, E. Gallo[16], J. Garay Garcia, A. Geiser, A. Gizhko, J.M. Grados Luyando, A. Grohsjean, P. Gunnellini, A. Harb, J. Hauk, M. Hempel[17], H. Jung, A. Kalogeropoulos, M. Kasemann, J. Keaveney, C. Kleinwort, I. Korol, D. Krücker, W. Lange, A. Lelek, T. Lenz, J. Leonard, K. Lipka, W. Lohmann[17], R. Mankel, I.-A. Melzer-Pellmann, A.B. Meyer, G. Mittag, J. Mnich, A. Mussgiller, E. Ntomari, D. Pitzl, R. Placakyte, A. Raspereza, B. Roland, M. Savitskyi, P. Saxena, R. Shevchenko, S. Spannagel, N. Stefaniuk, G.P. Van Onsem, R. Walsh, Y. Wen, K. Wichmann, C. Wissing, O. Zenaiev

University of Hamburg, Hamburg, Germany

S. Bein, V. Blobel, M. Centis Vignali, A.R. Draeger, T. Dreyer, E. Garutti, D. Gonzalez, J. Haller, M. Hoffmann, A. Junkes, R. Klanner, R. Kogler, N. Kovalchuk, S. Kurz, T. Lapsien, I. Marchesini, D. Marconi, M. Meyer, M. Niedziela, D. Nowatschin, F. Pantaleo[14], T. Peiffer, A. Perieanu, C. Scharf, P. Schleper, A. Schmidt, S. Schumann, J. Schwandt, J. Sonneveld, H. Stadie, G. Steinbrück, F.M. Stober, M. Stöver, H. Tholen, D. Troendle, E. Usai, L. Vanelderen, A. Vanhoefer, B. Vormwald

JHEP04(2018)060

Institut für Experimentelle Kernphysik, Karlsruhe, Germany

M. Akbiyik, C. Barth, S. Baur, E. Butz, R. Caspart, T. Chwalek, F. Colombo, W. De Boer, A. Dierlamm, B. Freund, R. Friese, M. Giffels, A. Gilbert, D. Haitz, F. Hartmann[14], S.M. Heindl, U. Husemann, F. Kassel[14], S. Kudella, H. Mildner, M.U. Mozer, Th. Müller, M. Plagge, G. Quast, K. Rabbertz, M. Schröder, I. Shvetsov, G. Sieber, H.J. Simonis, R. Ulrich, S. Wayand, M. Weber, T. Weiler, S. Williamson, C. Wöhrmann, R. Wolf

Institute of Nuclear and Particle Physics (INPP), NCSR Demokritos, Aghia Paraskevi, Greece

G. Anagnostou, G. Daskalakis, T. Geralis, V.A. Giakoumopoulou, A. Kyriakis, D. Loukas, I. Topsis-Giotis

National and Kapodistrian University of Athens, Athens, Greece

S. Kesisoglou, A. Panagiotou, N. Saoulidou

University of Ioánnina, Ioánnina, Greece

I. Evangelou, C. Foudas, P. Kokkas, N. Manthos, I. Papadopoulos, E. Paradas, J. Strologas, F.A. Triantis

MTA-ELTE Lendület CMS Particle and Nuclear Physics Group, Eötvös Loránd University, Budapest, Hungary

M. Csanad, N. Filipovic, G. Pasztor

Wigner Research Centre for Physics, Budapest, Hungary

G. Bencze, C. Hajdu, D. Horvath[18], F. Sikler, V. Veszpremi, G. Vesztergombi[19], A.J. Zsigmond

Institute of Nuclear Research ATOMKI, Debrecen, Hungary

N. Beni, S. Czellar, J. Karancsi[20], A. Makovec, J. Molnar, Z. Szillasi

Institute of Physics, University of Debrecen, Debrecen, Hungary

M. Bartók[19], P. Raics, Z.L. Trocsanyi, B. Ujvari

Indian Institute of Science (IISc), Bangalore, India

S. Choudhury, J.R. Komaragiri

National Institute of Science Education and Research, Bhubaneswar, India

S. Bahinipati[21], S. Bhowmik, P. Mal, K. Mandal, A. Nayak[22], D.K. Sahoo[21], N. Sahoo, S.K. Swain

Panjab University, Chandigarh, India

S. Bansal, S.B. Beri, V. Bhatnagar, U. Bhawandeep, R. Chawla, N. Dhingra, A.K. Kalsi, A. Kaur, M. Kaur, R. Kumar, P. Kumari, A. Mehta, M. Mittal, J.B. Singh, G. Walia

University of Delhi, Delhi, India

Ashok Kumar, Aashaq Shah, A. Bhardwaj, S. Chauhan, B.C. Choudhary, R.B. Garg, S. Keshri, A. Kumar, S. Malhotra, M. Naimuddin, K. Ranjan, R. Sharma, V. Sharma

JHEP04(2018)060

Saha Institute of Nuclear Physics, HBNI, Kolkata, India

R. Bhardwaj, R. Bhattacharya, S. Bhattacharya, S. Dey, S. Dutt, S. Dutta, S. Ghosh, N. Majumdar, A. Modak, K. Mondal, S. Mukhopadhyay, S. Nandan, A. Purohit, A. Roy, D. Roy, S. Roy Chowdhury, S. Sarkar, M. Sharan, S. Thakur

Indian Institute of Technology Madras, Madras, India

P.K. Behera

Bhabha Atomic Research Centre, Mumbai, India

R. Chudasama, D. Dutta, V. Jha, V. Kumar, A.K. Mohanty[14], P.K. Netrakanti, L.M. Pant, P. Shukla, A. Topkar

Tata Institute of Fundamental Research-A, Mumbai, India

T. Aziz, S. Dugad, B. Mahakud, S. Mitra, G.B. Mohanty, B. Parida, N. Sur, B. Sutar

Tata Institute of Fundamental Research-B, Mumbai, India

S. Banerjee, S. Bhattacharya, S. Chatterjee, P. Das, M. Guchait, Sa. Jain, S. Kumar, M. Maity[23], G. Majumder, K. Mazumdar, T. Sarkar[23], N. Wickramage[24]

Indian Institute of Science Education and Research (IISER), Pune, India

S. Chauhan, S. Dube, V. Hegde, A. Kapoor, K. Kothekar, S. Pandey, A. Rane, S. Sharma

Institute for Research in Fundamental Sciences (IPM), Tehran, Iran

S. Chenarani[25], E. Eskandari Tadavani, S.M. Etesami[25], M. Khakzad, M. Mohammadi Najafabadi, M. Naseri, S. Paktinat Mehdiabadi[26], F. Rezaei Hosseinabadi, B. Safarzadeh[27], M. Zeinali

University College Dublin, Dublin, Ireland

M. Felcini, M. Grunewald

INFN Sezione di Bari [a], Università di Bari [b], Politecnico di Bari [c], Bari, Italy

M. Abbrescia[a,b], C. Calabria[a,b], C. Caputo[a,b], A. Colaleo[a], D. Creanza[a,c], L. Cristella[a,b], N. De Filippis[a,c], M. De Palma[a,b], F. Errico[a,b], L. Fiore[a], G. Iaselli[a,c], G. Maggi[a,c], M. Maggi[a], G. Miniello[a,b], S. My[a,b], S. Nuzzo[a,b], A. Pompili[a,b], G. Pugliese[a,c], R. Radogna[a,b], A. Ranieri[a], G. Selvaggi[a,b], A. Sharma[a], L. Silvestris[a,14], R. Venditti[a], P. Verwilligen[a]

INFN Sezione di Bologna [a], Università di Bologna [b], Bologna, Italy

G. Abbiendi[a], C. Battilana, D. Bonacorsi[a,b], S. Braibant-Giacomelli[a,b], L. Brigliadori[a,b], R. Campanini[a,b], P. Capiluppi[a,b], A. Castro[a,b], F.R. Cavallo[a], S.S. Chhibra[a,b], G. Codispoti[a,b], M. Cuffiani[a,b], G.M. Dallavalle[a], F. Fabbri[a], A. Fanfani[a,b], D. Fasanella[a,b], P. Giacomelli[a], L. Guiducci[a,b], S. Marcellini[a], G. Masetti[a], F.L. Navarria[a,b], A. Perrotta[a], A.M. Rossi[a,b], T. Rovelli[a,b], G.P. Siroli[a,b], N. Tosi[a,b,14]

INFN Sezione di Catania [a], Università di Catania [b], Catania, Italy

S. Albergo[a,b], S. Costa[a,b], A. Di Mattia[a], F. Giordano[a,b], R. Potenza[a,b], A. Tricomi[a,b], C. Tuve[a,b]

JHEP04(2018)060

INFN Sezione di Firenze [a], Università di Firenze [b], Firenze, Italy
G. Barbagli[a], K. Chatterjee[a,b], V. Ciulli[a,b], C. Civinini[a], R. D'Alessandro[a,b], E. Focardi[a,b], P. Lenzi[a,b], M. Meschini[a], S. Paoletti[a], L. Russo[a,28], G. Sguazzoni[a], D. Strom[a], L. Viliani[a,b,14]

INFN Laboratori Nazionali di Frascati, Frascati, Italy
L. Benussi, S. Bianco, F. Fabbri, D. Piccolo, F. Primavera[14]

INFN Sezione di Genova [a], Università di Genova [b], Genova, Italy
V. Calvelli[a,b], F. Ferro[a], E. Robutti[a], S. Tosi[a,b]

INFN Sezione di Milano-Bicocca [a], Università di Milano-Bicocca [b], Milano, Italy
L. Brianza[a,b], F. Brivio[a,b], V. Ciriolo[a,b], M.E. Dinardo[a,b], S. Fiorendi[a,b], S. Gennai[a], A. Ghezzi[a,b], P. Govoni[a,b], M. Malberti[a,b], S. Malvezzi[a], R.A. Manzoni[a,b], D. Menasce[a], L. Moroni[a], M. Paganoni[a,b], K. Pauwels[a,b], D. Pedrini[a], S. Pigazzini[a,b,29], S. Ragazzi[a,b], T. Tabarelli de Fatis[a,b]

INFN Sezione di Napoli [a], Università di Napoli 'Federico II' [b], Napoli, Italy, Università della Basilicata [c], Potenza, Italy, Università G. Marconi [d], Roma, Italy
S. Buontempo[a], N. Cavallo[a,c], S. Di Guida[a,d,14], M. Esposito[a,b], F. Fabozzi[a,c], F. Fienga[a,b], A.O.M. Iorio[a,b], W.A. Khan[a], G. Lanza[a], L. Lista[a], S. Meola[a,d,14], P. Paolucci[a,14], C. Sciacca[a,b], F. Thyssen[a]

INFN Sezione di Padova [a], Università di Padova [b], Padova, Italy, Università di Trento [c], Trento, Italy
P. Azzi[a,14], N. Bacchetta[a], L. Benato[a,b], D. Bisello[a,b], A. Boletti[a,b], R. Carlin[a,b], A. Carvalho Antunes De Oliveira[a,b], P. Checchia[a], M. Dall'Osso[a,b], P. De Castro Manzano[a], T. Dorigo[a], F. Gasparini[a,b], U. Gasparini[a,b], A. Gozzelino[a], S. Lacaprara[a], M. Margoni[a,b], A.T. Meneguzzo[a,b], M. Passaseo[a], M. Pegoraro[a], N. Pozzobon[a,b], P. Ronchese[a,b], R. Rossin[a,b], F. Simonetto[a,b], E. Torassa[a], M. Zanetti[a,b], P. Zotto[a,b]

INFN Sezione di Pavia [a], Università di Pavia [b], Pavia, Italy
A. Braghieri[a], F. Fallavollita[a,b], A. Magnani[a,b], P. Montagna[a,b], S.P. Ratti[a,b], V. Re[a], M. Ressegotti, C. Riccardi[a,b], P. Salvini[a], I. Vai[a,b], P. Vitulo[a,b]

INFN Sezione di Perugia [a], Università di Perugia [b], Perugia, Italy
L. Alunni Solestizi[a,b], G.M. Bilei[a], D. Ciangottini[a,b], L. Fanò[a,b], P. Lariccia[a,b], R. Leonardi[a,b], G. Mantovani[a,b], V. Mariani[a,b], M. Menichelli[a], A. Saha[a], A. Santocchia[a,b], D. Spiga

INFN Sezione di Pisa [a], Università di Pisa [b], Scuola Normale Superiore di Pisa [c], Pisa, Italy
K. Androsov[a], P. Azzurri[a,14], G. Bagliesi[a], J. Bernardini[a], T. Boccali[a], L. Borrello, R. Castaldi[a], M.A. Ciocci[a,b], R. Dell'Orso[a], G. Fedi[a], A. Giassi[a], M.T. Grippo[a,28], F. Ligabue[a,c], T. Lomtadze[a], L. Martini[a,b], A. Messineo[a,b], F. Palla[a], A. Rizzi[a,b], A. Savoy-Navarro[a,30], P. Spagnolo[a], R. Tenchini[a], G. Tonelli[a,b], A. Venturi[a], P.G. Verdini[a]

JHEP04(2018)060

INFN Sezione di Roma [a], Sapienza Università di Roma [b], Rome, Italy

L. Barone[a,b], F. Cavallari[a], M. Cipriani[a,b], N. Daci[a], D. Del Re[a,b,14], M. Diemoz[a], S. Gelli[a,b], E. Longo[a,b], F. Margaroli[a,b], B. Marzocchi[a,b], P. Meridiani[a], G. Organtini[a,b], R. Paramatti[a,b], F. Preiato[a,b], S. Rahatlou[a,b], C. Rovelli[a], F. Santanastasio[a,b]

INFN Sezione di Torino [a], Università di Torino [b], Torino, Italy, Università del Piemonte Orientale [c], Novara, Italy

N. Amapane[a,b], R. Arcidiacono[a,c,14], S. Argiro[a,b], M. Arneodo[a,c], N. Bartosik[a], R. Bellan[a,b], C. Biino[a], N. Cartiglia[a], F. Cenna[a,b], M. Costa[a,b], R. Covarelli[a,b], A. Degano[a,b], N. Demaria[a], B. Kiani[a,b], C. Mariotti[a], S. Maselli[a], E. Migliore[a,b], V. Monaco[a,b], E. Monteil[a,b], M. Monteno[a], M.M. Obertino[a,b], L. Pacher[a,b], N. Pastrone[a], M. Pelliccioni[a], G.L. Pinna Angioni[a,b], F. Ravera[a,b], A. Romero[a,b], M. Ruspa[a,c], R. Sacchi[a,b], K. Shchelina[a,b], V. Sola[a], A. Solano[a,b], A. Staiano[a], P. Traczyk[a,b]

INFN Sezione di Trieste [a], Università di Trieste [b], Trieste, Italy

S. Belforte[a], M. Casarsa[a], F. Cossutti[a], G. Della Ricca[a,b], A. Zanetti[a]

Kyungpook National University, Daegu, Korea

D.H. Kim, G.N. Kim, M.S. Kim, J. Lee, S. Lee, S.W. Lee, Y.D. Oh, S. Sekmen, D.C. Son, Y.C. Yang

Chonbuk National University, Jeonju, Korea

A. Lee

Chonnam National University, Institute for Universe and Elementary Particles, Kwangju, Korea

H. Kim, D.H. Moon, G. Oh

Hanyang University, Seoul, Korea

J.A. Brochero Cifuentes, J. Goh, T.J. Kim

Korea University, Seoul, Korea

S. Cho, S. Choi, Y. Go, D. Gyun, S. Ha, B. Hong, Y. Jo, Y. Kim, K. Lee, K.S. Lee, S. Lee, J. Lim, S.K. Park, Y. Roh

Seoul National University, Seoul, Korea

J. Almond, J. Kim, J.S. Kim, H. Lee, K. Lee, K. Nam, S.B. Oh, B.C. Radburn-Smith, S.h. Seo, U.K. Yang, H.D. Yoo, G.B. Yu

University of Seoul, Seoul, Korea

M. Choi, H. Kim, J.H. Kim, J.S.H. Lee, I.C. Park, G. Ryu

Sungkyunkwan University, Suwon, Korea

Y. Choi, C. Hwang, J. Lee, I. Yu

Vilnius University, Vilnius, Lithuania

V. Dudenas, A. Juodagalvis, J. Vaitkus

JHEP04(2018)060

National Centre for Particle Physics, Universiti Malaya, Kuala Lumpur, Malaysia

I. Ahmed, Z.A. Ibrahim, M.A.B. Md Ali[31], F. Mohamad Idris[32], W.A.T. Wan Abdullah, M.N. Yusli, Z. Zolkapli

Centro de Investigacion y de Estudios Avanzados del IPN, Mexico City, Mexico

H. Castilla-Valdez, E. De La Cruz-Burelo, I. Heredia-De La Cruz[33], R. Lopez-Fernandez, J. Mejia Guisao, A. Sanchez-Hernandez

Universidad Iberoamericana, Mexico City, Mexico

S. Carrillo Moreno, C. Oropeza Barrera, F. Vazquez Valencia

Benemerita Universidad Autonoma de Puebla, Puebla, Mexico

I. Pedraza, H.A. Salazar Ibarguen, C. Uribe Estrada

Universidad Autónoma de San Luis Potosí, San Luis Potosí, Mexico

A. Morelos Pineda

University of Auckland, Auckland, New Zealand

D. Krofcheck

University of Canterbury, Christchurch, New Zealand

P.H. Butler

National Centre for Physics, Quaid-I-Azam University, Islamabad, Pakistan

A. Ahmad, M. Ahmad, Q. Hassan, H.R. Hoorani, A. Saddique, M.A. Shah, M. Shoaib, M. Waqas

National Centre for Nuclear Research, Swierk, Poland

H. Bialkowska, M. Bluj, B. Boimska, T. Frueboes, M. Górski, M. Kazana, K. Nawrocki, K. Romanowska-Rybinska, M. Szleper, P. Zalewski

Institute of Experimental Physics, Faculty of Physics, University of Warsaw, Warsaw, Poland

K. Bunkowski, A. Byszuk[34], K. Doroba, A. Kalinowski, M. Konecki, J. Krolikowski, M. Misiura, M. Olszewski, A. Pyskir, M. Walczak

Laboratório de Instrumentação e Física Experimental de Partículas, Lisboa, Portugal

P. Bargassa, C. Beirão Da Cruz E Silva, B. Calpas, A. Di Francesco, P. Faccioli, M. Gallinaro, J. Hollar, N. Leonardo, L. Lloret Iglesias, M.V. Nemallapudi, J. Seixas, O. Toldaiev, D. Vadruccio, J. Varela

Joint Institute for Nuclear Research, Dubna, Russia

S. Afanasiev, P. Bunin, M. Gavrilenko, I. Golutvin, I. Gorbunov, A. Kamenev, V. Karjavin, A. Lanev, A. Malakhov, V. Matveev[35,36], V. Palichik, V. Perelygin, S. Shmatov, S. Shulha, N. Skatchkov, V. Smirnov, N. Voytishin, A. Zarubin

JHEP04(2018)060

Petersburg Nuclear Physics Institute, Gatchina (St. Petersburg), Russia
Y. Ivanov, V. Kim[37], E. Kuznetsova[38], P. Levchenko, V. Murzin, V. Oreshkin, I. Smirnov, V. Sulimov, L. Uvarov, S. Vavilov, A. Vorobyev

Institute for Nuclear Research, Moscow, Russia
Yu. Andreev, A. Dermenev, S. Gninenko, N. Golubev, A. Karneyeu, M. Kirsanov, N. Krasnikov, A. Pashenkov, D. Tlisov, A. Toropin

Institute for Theoretical and Experimental Physics, Moscow, Russia
V. Epshteyn, V. Gavrilov, N. Lychkovskaya, V. Popov, I. Pozdnyakov, G. Safronov, A. Spiridonov, A. Stepennov, M. Toms, E. Vlasov, A. Zhokin

Moscow Institute of Physics and Technology, Moscow, Russia
T. Aushev, A. Bylinkin[36]

National Research Nuclear University 'Moscow Engineering Physics Institute' (MEPhI), Moscow, Russia
M. Danilov[39], P. Parygin, E. Tarkovskii

P.N. Lebedev Physical Institute, Moscow, Russia
V. Andreev, M. Azarkin[36], I. Dremin[36], M. Kirakosyan, A. Terkulov

Skobeltsyn Institute of Nuclear Physics, Lomonosov Moscow State University, Moscow, Russia
A. Baskakov, A. Belyaev, E. Boos, V. Bunichev, M. Dubinin[40], L. Dudko, V. Klyukhin, O. Kodolova, N. Korneeva, I. Lokhtin, I. Miagkov, S. Obraztsov, M. Perfilov, V. Savrin, P. Volkov

Novosibirsk State University (NSU), Novosibirsk, Russia
V. Blinov[41], Y.Skovpen[41], D. Shtol[41]

State Research Center of Russian Federation, Institute for High Energy Physics, Protvino, Russia
I. Azhgirey, I. Bayshev, S. Bitioukov, D. Elumakhov, V. Kachanov, A. Kalinin, D. Konstantinov, V. Krychkine, V. Petrov, R. Ryutin, A. Sobol, S. Troshin, N. Tyurin, A. Uzunian, A. Volkov

University of Belgrade, Faculty of Physics and Vinca Institute of Nuclear Sciences, Belgrade, Serbia
P. Adzic[42], P. Cirkovic, D. Devetak, M. Dordevic, J. Milosevic, V. Rekovic

Centro de Investigaciones Energéticas Medioambientales y Tecnológicas (CIEMAT), Madrid, Spain
J. Alcaraz Maestre, M. Barrio Luna, M. Cerrada, N. Colino, B. De La Cruz, A. Delgado Peris, A. Escalante Del Valle, C. Fernandez Bedoya, J.P. Fernández Ramos, J. Flix, M.C. Fouz, P. Garcia-Abia, O. Gonzalez Lopez, S. Goy Lopez, J.M. Hernandez, M.I. Josa, A. Pérez-Calero Yzquierdo, J. Puerta Pelayo, A. Quintario Olmeda, I. Redondo, L. Romero, M.S. Soares, A. Álvarez Fernández

JHEP04(2018)060

Universidad Autónoma de Madrid, Madrid, Spain
J.F. de Trocóniz, M. Missiroli, D. Moran

Universidad de Oviedo, Oviedo, Spain
J. Cuevas, C. Erice, J. Fernandez Menendez, I. Gonzalez Caballero, J.R. González Fernández, E. Palencia Cortezon, S. Sanchez Cruz, I. Suárez Andrés, P. Vischia, J.M. Vizan Garcia

Instituto de Física de Cantabria (IFCA), CSIC-Universidad de Cantabria, Santander, Spain
I.J. Cabrillo, A. Calderon, B. Chazin Quero, E. Curras, M. Fernandez, J. Garcia-Ferrero, G. Gomez, A. Lopez Virto, J. Marco, C. Martinez Rivero, P. Martinez Ruiz del Arbol, F. Matorras, J. Piedra Gomez, T. Rodrigo, A. Ruiz-Jimeno, L. Scodellaro, N. Trevisani, I. Vila, R. Vilar Cortabitarte

CERN, European Organization for Nuclear Research, Geneva, Switzerland
D. Abbaneo, E. Auffray, P. Baillon, A.H. Ball, D. Barney, M. Bianco, P. Bloch, A. Bocci, C. Botta, T. Camporesi, R. Castello, M. Cepeda, G. Cerminara, E. Chapon, Y. Chen, D. d'Enterria, A. Dabrowski, V. Daponte, A. David, M. De Gruttola, A. De Roeck, E. Di Marco[43], M. Dobson, B. Dorney, T. du Pree, M. Dünser, N. Dupont, A. Elliott-Peisert, P. Everaerts, G. Franzoni, J. Fulcher, W. Funk, D. Gigi, K. Gill, F. Glege, D. Gulhan, S. Gundacker, M. Guthoff, P. Harris, J. Hegeman, V. Innocente, P. Janot, O. Karacheban[17], J. Kieseler, H. Kirschenmann, V. Knünz, A. Kornmayer[14], M.J. Kortelainen, M. Krammer[1], C. Lange, P. Lecoq, C. Lourenço, M.T. Lucchini, L. Malgeri, M. Mannelli, A. Martelli, F. Meijers, J.A. Merlin, S. Mersi, E. Meschi, P. Milenovic[44], F. Moortgat, M. Mulders, H. Neugebauer, S. Orfanelli, L. Orsini, L. Pape, E. Perez, M. Peruzzi, A. Petrilli, G. Petrucciani, A. Pfeiffer, M. Pierini, A. Racz, T. Reis, G. Rolandi[45], M. Rovere, H. Sakulin, C. Schäfer, C. Schwick, M. Seidel, M. Selvaggi, A. Sharma, P. Silva, P. Sphicas[46], J. Steggemann, M. Stoye, M. Tosi, D. Treille, A. Triossi, A. Tsirou, V. Veckalns[47], G.I. Veres[19], M. Verweij, N. Wardle, W.D. Zeuner

Paul Scherrer Institut, Villigen, Switzerland
W. Bertl†, K. Deiters, W. Erdmann, R. Horisberger, Q. Ingram, H.C. Kaestli, D. Kotlinski, U. Langenegger, T. Rohe, S.A. Wiederkehr

Institute for Particle Physics, ETH Zurich, Zurich, Switzerland
F. Bachmair, L. Bäni, P. Berger, L. Bianchini, B. Casal, G. Dissertori, M. Dittmar, M. Donegà, C. Grab, C. Heidegger, D. Hits, J. Hoss, G. Kasieczka, T. Klijnsma, W. Lustermann, B. Mangano, M. Marionneau, M.T. Meinhard, D. Meister, F. Micheli, P. Musella, F. Nessi-Tedaldi, F. Pandolfi, J. Pata, F. Pauss, G. Perrin, L. Perrozzi, M. Quittnat, M. Rossini, M. Schönenberger, L. Shchutska, A. Starodumov[48], V.R. Tavolaro, K. Theofilatos, M.L. Vesterbacka Olsson, R. Wallny, A. Zagozdzinska[34], D.H. Zhu

Universität Zürich, Zurich, Switzerland
T.K. Aarrestad, C. Amsler[49], L. Caminada, M.F. Canelli, A. De Cosa, S. Donato, C. Galloni, A. Hinzmann, T. Hreus, B. Kilminster, J. Ngadiuba, D. Pinna, G. Rauco,

JHEP04(2018)060

P. Robmann, D. Salerno, C. Seitz, A. Zucchetta

National Central University, Chung-Li, Taiwan

V. Candelise, T.H. Doan, Sh. Jain, R. Khurana, M. Konyushikhin, C.M. Kuo, W. Lin, A. Pozdnyakov, S.S. Yu

National Taiwan University (NTU), Taipei, Taiwan

Arun Kumar, P. Chang, Y. Chao, K.F. Chen, P.H. Chen, F. Fiori, W.-S. Hou, Y. Hsiung, Y.F. Liu, R.-S. Lu, M. Miñano Moya, E. Paganis, A. Psallidas, J.f. Tsai

Chulalongkorn University, Faculty of Science, Department of Physics, Bangkok, Thailand

B. Asavapibhop, K. Kovitanggoon, G. Singh, N. Srimanobhas

Çukurova University, Physics Department, Science and Art Faculty, Adana, Turkey

A. Adiguzel[50], F. Boran, S. Cerci[51], S. Damarseckin, Z.S. Demiroglu, C. Dozen, I. Dumanoglu, S. Girgis, G. Gokbulut, Y. Guler, I. Hos[52], E.E. Kangal[53], O. Kara, A. Kayis Topaksu, U. Kiminsu, M. Oglakci, G. Onengut[54], K. Ozdemir[55], D. Sunar Cerci[51], H. Topakli[56], S. Turkcapar, I.S. Zorbakir, C. Zorbilmez

Middle East Technical University, Physics Department, Ankara, Turkey

B. Bilin, G. Karapinar[57], K. Ocalan[58], M. Yalvac, M. Zeyrek

Bogazici University, Istanbul, Turkey

E. Gülmez, M. Kaya[59], O. Kaya[60], S. Tekten, E.A. Yetkin[61]

Istanbul Technical University, Istanbul, Turkey

M.N. Agaras, S. Atay, A. Cakir, K. Cankocak

Institute for Scintillation Materials of National Academy of Science of Ukraine, Kharkov, Ukraine

B. Grynyov

National Scientific Center, Kharkov Institute of Physics and Technology, Kharkov, Ukraine

L. Levchuk, P. Sorokin

University of Bristol, Bristol, United Kingdom

R. Aggleton, F. Ball, L. Beck, J.J. Brooke, D. Burns, E. Clement, D. Cussans, H. Flacher, J. Goldstein, M. Grimes, G.P. Heath, H.F. Heath, J. Jacob, L. Kreczko, C. Lucas, D.M. Newbold[62], S. Paramesvaran, A. Poll, T. Sakuma, S. Seif El Nasr-storey, D. Smith, V.J. Smith

Rutherford Appleton Laboratory, Didcot, United Kingdom

K.W. Bell, A. Belyaev[63], C. Brew, R.M. Brown, L. Calligaris, D. Cieri, D.J.A. Cockerill, J.A. Coughlan, K. Harder, S. Harper, E. Olaiya, D. Petyt, C.H. Shepherd-Themistocleous, A. Thea, I.R. Tomalin, T. Williams

JHEP04(2018)060

Imperial College, London, United Kingdom
M. Baber, R. Bainbridge, S. Breeze, O. Buchmuller, A. Bundock, S. Casasso, M. Citron, D. Colling, L. Corpe, P. Dauncey, G. Davies, A. De Wit, M. Della Negra, R. Di Maria, P. Dunne, A. Elwood, D. Futyan, Y. Haddad, G. Hall, G. Iles, T. James, R. Lane, C. Laner, L. Lyons, A.-M. Magnan, S. Malik, L. Mastrolorenzo, T. Matsushita, J. Nash, A. Nikitenko[48], J. Pela, M. Pesaresi, D.M. Raymond, A. Richards, A. Rose, E. Scott, C. Seez, A. Shtipliyski, S. Summers, A. Tapper, K. Uchida, M. Vazquez Acosta[64], T. Virdee[14], D. Winterbottom, J. Wright, S.C. Zenz

Brunel University, Uxbridge, United Kingdom
J.E. Cole, P.R. Hobson, A. Khan, P. Kyberd, I.D. Reid, P. Symonds, L. Teodorescu, M. Turner

Baylor University, Waco, U.S.A.
A. Borzou, K. Call, J. Dittmann, K. Hatakeyama, H. Liu, N. Pastika

Catholic University of America, Washington DC, U.S.A.
R. Bartek, A. Dominguez

The University of Alabama, Tuscaloosa, U.S.A.
A. Buccilli, S.I. Cooper, C. Henderson, P. Rumerio, C. West

Boston University, Boston, U.S.A.
D. Arcaro, A. Avetisyan, T. Bose, D. Gastler, D. Rankin, C. Richardson, J. Rohlf, L. Sulak, D. Zou

Brown University, Providence, U.S.A.
G. Benelli, D. Cutts, A. Garabedian, J. Hakala, U. Heintz, J.M. Hogan, K.H.M. Kwok, E. Laird, G. Landsberg, Z. Mao, M. Narain, J. Pazzini, S. Piperov, S. Sagir, R. Syarif, D. Yu

University of California, Davis, Davis, U.S.A.
R. Band, C. Brainerd, D. Burns, M. Calderon De La Barca Sanchez, M. Chertok, J. Conway, R. Conway, P.T. Cox, R. Erbacher, C. Flores, G. Funk, M. Gardner, W. Ko, R. Lander, C. Mclean, M. Mulhearn, D. Pellett, J. Pilot, S. Shalhout, M. Shi, J. Smith, M. Squires, D. Stolp, K. Tos, M. Tripathi, Z. Wang

University of California, Los Angeles, U.S.A.
M. Bachtis, C. Bravo, R. Cousins, A. Dasgupta, A. Florent, J. Hauser, M. Ignatenko, N. Mccoll, D. Saltzberg, C. Schnaible, V. Valuev

University of California, Riverside, Riverside, U.S.A.
E. Bouvier, K. Burt, R. Clare, J. Ellison, J.W. Gary, S.M.A. Ghiasi Shirazi, G. Hanson, J. Heilman, P. Jandir, E. Kennedy, F. Lacroix, O.R. Long, M. Olmedo Negrete, M.I. Paneva, A. Shrinivas, W. Si, H. Wei, S. Wimpenny, B. R. Yates

University of California, San Diego, La Jolla, U.S.A.
J.G. Branson, G.B. Cerati, S. Cittolin, M. Derdzinski, R. Gerosa, B. Hashemi, A. Holzner, D. Klein, G. Kole, V. Krutelyov, J. Letts, I. Macneill, M. Masciovecchio, D. Olivito,

JHEP04(2018)060

S. Padhi, M. Pieri, M. Sani, V. Sharma, S. Simon, M. Tadel, A. Vartak, S. Wasserbaech[65], J. Wood, F. Würthwein, A. Yagil, G. Zevi Della Porta

University of California, Santa Barbara - Department of Physics, Santa Barbara, U.S.A.

N. Amin, R. Bhandari, J. Bradmiller-Feld, C. Campagnari, A. Dishaw, V. Dutta, M. Franco Sevilla, C. George, F. Golf, L. Gouskos, J. Gran, R. Heller, J. Incandela, S.D. Mullin, A. Ovcharova, H. Qu, J. Richman, D. Stuart, I. Suarez, J. Yoo

California Institute of Technology, Pasadena, U.S.A.

D. Anderson, J. Bendavid, A. Bornheim, J.M. Lawhorn, H.B. Newman, T. Nguyen, C. Pena, M. Spiropulu, J.R. Vlimant, S. Xie, Z. Zhang, R.Y. Zhu

Carnegie Mellon University, Pittsburgh, U.S.A.

M.B. Andrews, T. Ferguson, T. Mudholkar, M. Paulini, J. Russ, M. Sun, H. Vogel, I. Vorobiev, M. Weinberg

University of Colorado Boulder, Boulder, U.S.A.

J.P. Cumalat, W.T. Ford, F. Jensen, A. Johnson, M. Krohn, S. Leontsinis, T. Mulholland, K. Stenson, S.R. Wagner

Cornell University, Ithaca, U.S.A.

J. Alexander, J. Chaves, J. Chu, S. Dittmer, K. Mcdermott, N. Mirman, J.R. Patterson, A. Rinkevicius, A. Ryd, L. Skinnari, L. Soffi, S.M. Tan, Z. Tao, J. Thom, J. Tucker, P. Wittich, M. Zientek

Fermi National Accelerator Laboratory, Batavia, U.S.A.

S. Abdullin, M. Albrow, G. Apollinari, A. Apresyan, A. Apyan, S. Banerjee, L.A.T. Bauerdick, A. Beretvas, J. Berryhill, P.C. Bhat, G. Bolla, K. Burkett, J.N. Butler, A. Canepa, H.W.K. Cheung, F. Chlebana, M. Cremonesi, J. Duarte, V.D. Elvira, J. Freeman, Z. Gecse, E. Gottschalk, L. Gray, D. Green, S. Grünendahl, O. Gutsche, R.M. Harris, S. Hasegawa, J. Hirschauer, Z. Hu, B. Jayatilaka, S. Jindariani, M. Johnson, U. Joshi, B. Klima, B. Kreis, S. Lammel, D. Lincoln, R. Lipton, M. Liu, T. Liu, R. Lopes De Sá, J. Lykken, K. Maeshima, N. Magini, J.M. Marraffino, S. Maruyama, D. Mason, P. McBride, P. Merkel, S. Mrenna, S. Nahn, V. O'Dell, K. Pedro, O. Prokofyev, G. Rakness, L. Ristori, B. Schneider, E. Sexton-Kennedy, A. Soha, W.J. Spalding, L. Spiegel, S. Stoynev, J. Strait, N. Strobbe, L. Taylor, S. Tkaczyk, N.V. Tran, L. Uplegger, E.W. Vaandering, C. Vernieri, M. Verzocchi, R. Vidal, M. Wang, H.A. Weber, A. Whitbeck

University of Florida, Gainesville, U.S.A.

D. Acosta, P. Avery, P. Bortignon, A. Brinkerhoff, A. Carnes, M. Carver, D. Curry, S. Das, R.D. Field, I.K. Furic, J. Konigsberg, A. Korytov, K. Kotov, P. Ma, K. Matchev, H. Mei, G. Mitselmakher, D. Rank, D. Sperka, N. Terentyev, L. Thomas, J. Wang, S. Wang, J. Yelton

Florida International University, Miami, U.S.A.

Y.R. Joshi, S. Linn, P. Markowitz, G. Martinez, J.L. Rodriguez

JHEP04(2018)060

Florida State University, Tallahassee, U.S.A.

A. Ackert, T. Adams, A. Askew, S. Hagopian, V. Hagopian, K.F. Johnson, T. Kolberg, T. Perry, H. Prosper, A. Santra, R. Yohay

Florida Institute of Technology, Melbourne, U.S.A.

M.M. Baarmand, V. Bhopatkar, S. Colafranceschi, M. Hohlmann, D. Noonan, T. Roy, F. Yumiceva

University of Illinois at Chicago (UIC), Chicago, U.S.A.

M.R. Adams, L. Apanasevich, D. Berry, R.R. Betts, R. Cavanaugh, X. Chen, O. Evdokimov, C.E. Gerber, D.A. Hangal, D.J. Hofman, K. Jung, J. Kamin, I.D. Sandoval Gonzalez, M.B. Tonjes, H. Trauger, N. Varelas, H. Wang, Z. Wu, J. Zhang

The University of Iowa, Iowa City, U.S.A.

B. Bilki[66], W. Clarida, K. Dilsiz[67], S. Durgut, R.P. Gandrajula, M. Haytmyradov, V. Khristenko, J.-P. Merlo, H. Mermerkaya[68], A. Mestvirishvili, A. Moeller, J. Nachtman, H. Ogul[69], Y. Onel, F. Ozok[70], A. Penzo, C. Snyder, E. Tiras, J. Wetzel, K. Yi

Johns Hopkins University, Baltimore, U.S.A.

B. Blumenfeld, A. Cocoros, N. Eminizer, D. Fehling, L. Feng, A.V. Gritsan, P. Maksimovic, J. Roskes, U. Sarica, M. Swartz, M. Xiao, C. You

The University of Kansas, Lawrence, U.S.A.

A. Al-bataineh, P. Baringer, A. Bean, S. Boren, J. Bowen, J. Castle, S. Khalil, A. Kropivnitskaya, D. Majumder, W. Mcbrayer, M. Murray, C. Royon, S. Sanders, E. Schmitz, R. Stringer, J.D. Tapia Takaki, Q. Wang

Kansas State University, Manhattan, U.S.A.

A. Ivanov, K. Kaadze, Y. Maravin, A. Mohammadi, L.K. Saini, N. Skhirtladze, S. Toda

Lawrence Livermore National Laboratory, Livermore, U.S.A.

F. Rebassoo, D. Wright

University of Maryland, College Park, U.S.A.

C. Anelli, A. Baden, O. Baron, A. Belloni, B. Calvert, S.C. Eno, C. Ferraioli, N.J. Hadley, S. Jabeen, G.Y. Jeng, R.G. Kellogg, J. Kunkle, A.C. Mignerey, F. Ricci-Tam, Y.H. Shin, A. Skuja, S.C. Tonwar

Massachusetts Institute of Technology, Cambridge, U.S.A.

D. Abercrombie, B. Allen, V. Azzolini, R. Barbieri, A. Baty, R. Bi, S. Brandt, W. Busza, I.A. Cali, M. D'Alfonso, Z. Demiragli, G. Gomez Ceballos, M. Goncharov, D. Hsu, Y. Iiyama, G.M. Innocenti, M. Klute, D. Kovalskyi, Y.S. Lai, Y.-J. Lee, A. Levin, P.D. Luckey, B. Maier, A.C. Marini, C. Mcginn, C. Mironov, S. Narayanan, X. Niu, C. Paus, C. Roland, G. Roland, J. Salfeld-Nebgen, G.S.F. Stephans, K. Tatar, D. Velicanu, J. Wang, T.W. Wang, B. Wyslouch

University of Minnesota, Minneapolis, U.S.A.

A.C. Benvenuti, R.M. Chatterjee, A. Evans, P. Hansen, S. Kalafut, Y. Kubota, Z. Lesko, J. Mans, S. Nourbakhsh, N. Ruckstuhl, R. Rusack, J. Turkewitz

JHEP04(2018)060

University of Mississippi, Oxford, U.S.A.
J.G. Acosta, S. Oliveros

University of Nebraska-Lincoln, Lincoln, U.S.A.
E. Avdeeva, K. Bloom, D.R. Claes, C. Fangmeier, R. Gonzalez Suarez, R. Kamalieddin, I. Kravchenko, J. Monroy, J.E. Siado, G.R. Snow, B. Stieger

State University of New York at Buffalo, Buffalo, U.S.A.
M. Alyari, J. Dolen, A. Godshalk, C. Harrington, I. Iashvili, D. Nguyen, A. Parker, S. Rappoccio, B. Roozbahani

Northeastern University, Boston, U.S.A.
G. Alverson, E. Barberis, A. Hortiangtham, A. Massironi, D.M. Morse, D. Nash, T. Orimoto, R. Teixeira De Lima, D. Trocino, R.-J. Wang, D. Wood

Northwestern University, Evanston, U.S.A.
S. Bhattacharya, O. Charaf, K.A. Hahn, N. Mucia, N. Odell, B. Pollack, M.H. Schmitt, K. Sung, M. Trovato, M. Velasco

University of Notre Dame, Notre Dame, U.S.A.
N. Dev, M. Hildreth, K. Hurtado Anampa, C. Jessop, D.J. Karmgard, N. Kellams, K. Lannon, N. Loukas, N. Marinelli, F. Meng, C. Mueller, Y. Musienko[35], M. Planer, A. Reinsvold, R. Ruchti, G. Smith, S. Taroni, M. Wayne, M. Wolf, A. Woodard

The Ohio State University, Columbus, U.S.A.
J. Alimena, L. Antonelli, B. Bylsma, L.S. Durkin, S. Flowers, B. Francis, A. Hart, C. Hill, W. Ji, B. Liu, W. Luo, D. Puigh, B.L. Winer, H.W. Wulsin

Princeton University, Princeton, U.S.A.
A. Benaglia, S. Cooperstein, O. Driga, P. Elmer, J. Hardenbrook, P. Hebda, D. Lange, J. Luo, D. Marlow, K. Mei, I. Ojalvo, J. Olsen, C. Palmer, P. Piroué, D. Stickland, A. Svyatkovskiy, C. Tully

University of Puerto Rico, Mayaguez, U.S.A.
S. Malik, S. Norberg

Purdue University, West Lafayette, U.S.A.
A. Barker, V.E. Barnes, S. Folgueras, L. Gutay, M.K. Jha, M. Jones, A.W. Jung, A. Khatiwada, D.H. Miller, N. Neumeister, J.F. Schulte, J. Sun, F. Wang, W. Xie

Purdue University Northwest, Hammond, U.S.A.
T. Cheng, N. Parashar, J. Stupak

Rice University, Houston, U.S.A.
A. Adair, B. Akgun, Z. Chen, K.M. Ecklund, F.J.M. Geurts, M. Guilbaud, W. Li, B. Michlin, M. Northup, B.P. Padley, J. Roberts, J. Rorie, Z. Tu, J. Zabel

University of Rochester, Rochester, U.S.A.
A. Bodek, P. de Barbaro, R. Demina, Y.t. Duh, T. Ferbel, M. Galanti, A. Garcia-Bellido, J. Han, O. Hindrichs, A. Khukhunaishvili, K.H. Lo, P. Tan, M. Verzetti

JHEP04(2018)060

The Rockefeller University, New York, U.S.A.
R. Ciesielski, K. Goulianos, C. Mesropian

Rutgers, The State University of New Jersey, Piscataway, U.S.A.
A. Agapitos, J.P. Chou, Y. Gershtein, T.A. Gómez Espinosa, E. Halkiadakis, M. Heindl, E. Hughes, S. Kaplan, R. Kunnawalkam Elayavalli, S. Kyriacou, A. Lath, R. Montalvo, K. Nash, M. Osherson, H. Saka, S. Salur, S. Schnetzer, D. Sheffield, S. Somalwar, R. Stone, S. Thomas, P. Thomassen, M. Walker

University of Tennessee, Knoxville, U.S.A.
M. Foerster, J. Heideman, G. Riley, K. Rose, S. Spanier, K. Thapa

Texas A&M University, College Station, U.S.A.
O. Bouhali[71], A. Castaneda Hernandez[71], A. Celik, M. Dalchenko, M. De Mattia, A. Delgado, S. Dildick, R. Eusebi, J. Gilmore, T. Huang, T. Kamon[72], R. Mueller, Y. Pakhotin, R. Patel, A. Perloff, L. Perniè, D. Rathjens, A. Safonov, A. Tatarinov, K.A. Ulmer

Texas Tech University, Lubbock, U.S.A.
N. Akchurin, J. Damgov, F. De Guio, P.R. Dudero, J. Faulkner, E. Gurpinar, S. Kunori, K. Lamichhane, S.W. Lee, T. Libeiro, T. Peltola, S. Undleeb, I. Volobouev, Z. Wang

Vanderbilt University, Nashville, U.S.A.
S. Greene, A. Gurrola, R. Janjam, W. Johns, C. Maguire, A. Melo, H. Ni, P. Sheldon, S. Tuo, J. Velkovska, Q. Xu

University of Virginia, Charlottesville, U.S.A.
M.W. Arenton, P. Barria, B. Cox, R. Hirosky, A. Ledovskoy, H. Li, C. Neu, T. Sinthuprasith, X. Sun, Y. Wang, E. Wolfe, F. Xia

Wayne State University, Detroit, U.S.A.
C. Clarke, R. Harr, P.E. Karchin, J. Sturdy, S. Zaleski

University of Wisconsin - Madison, Madison, WI, U.S.A.
J. Buchanan, C. Caillol, S. Dasu, L. Dodd, S. Duric, B. Gomber, M. Grothe, M. Herndon, A. Hervé, U. Hussain, P. Klabbers, A. Lanaro, A. Levine, K. Long, R. Loveless, G.A. Pierro, G. Polese, T. Ruggles, A. Savin, N. Smith, W.H. Smith, D. Taylor, N. Woods

†: Deceased
1: Also at Vienna University of Technology, Vienna, Austria
2: Also at State Key Laboratory of Nuclear Physics and Technology, Peking University, Beijing, China
3: Also at Universidade Estadual de Campinas, Campinas, Brazil
4: Also at Universidade Federal de Pelotas, Pelotas, Brazil
5: Also at Université Libre de Bruxelles, Bruxelles, Belgium
6: Also at Joint Institute for Nuclear Research, Dubna, Russia
7: Also at Helwan University, Cairo, Egypt
8: Now at Zewail City of Science and Technology, Zewail, Egypt
9: Now at Fayoum University, El-Fayoum, Egypt

JHEP04(2018)060

10: Also at British University in Egypt, Cairo, Egypt
11: Now at Ain Shams University, Cairo, Egypt
12: Also at Université de Haute Alsace, Mulhouse, France
13: Also at Skobeltsyn Institute of Nuclear Physics, Lomonosov Moscow State University, Moscow, Russia
14: Also at CERN, European Organization for Nuclear Research, Geneva, Switzerland
15: Also at RWTH Aachen University, III. Physikalisches Institut A, Aachen, Germany
16: Also at University of Hamburg, Hamburg, Germany
17: Also at Brandenburg University of Technology, Cottbus, Germany
18: Also at Institute of Nuclear Research ATOMKI, Debrecen, Hungary
19: Also at MTA-ELTE Lendület CMS Particle and Nuclear Physics Group, Eötvös Loránd University, Budapest, Hungary
20: Also at Institute of Physics, University of Debrecen, Debrecen, Hungary
21: Also at Indian Institute of Technology Bhubaneswar, Bhubaneswar, India
22: Also at Institute of Physics, Bhubaneswar, India
23: Also at University of Visva-Bharati, Santiniketan, India
24: Also at University of Ruhuna, Matara, Sri Lanka
25: Also at Isfahan University of Technology, Isfahan, Iran
26: Also at Yazd University, Yazd, Iran
27: Also at Plasma Physics Research Center, Science and Research Branch, Islamic Azad University, Tehran, Iran
28: Also at Università degli Studi di Siena, Siena, Italy
29: Also at INFN Sezione di Milano-Bicocca; Università di Milano-Bicocca, Milano, Italy
30: Also at Purdue University, West Lafayette, U.S.A.
31: Also at International Islamic University of Malaysia, Kuala Lumpur, Malaysia
32: Also at Malaysian Nuclear Agency, MOSTI, Kajang, Malaysia
33: Also at Consejo Nacional de Ciencia y Tecnología, Mexico city, Mexico
34: Also at Warsaw University of Technology, Institute of Electronic Systems, Warsaw, Poland
35: Also at Institute for Nuclear Research, Moscow, Russia
36: Now at National Research Nuclear University 'Moscow Engineering Physics Institute' (MEPhI), Moscow, Russia
37: Also at St. Petersburg State Polytechnical University, St. Petersburg, Russia
38: Also at University of Florida, Gainesville, U.S.A.
39: Also at P.N. Lebedev Physical Institute, Moscow, Russia
40: Also at California Institute of Technology, Pasadena, U.S.A.
41: Also at Budker Institute of Nuclear Physics, Novosibirsk, Russia
42: Also at Faculty of Physics, University of Belgrade, Belgrade, Serbia
43: Also at INFN Sezione di Roma; Sapienza Università di Roma, Rome, Italy
44: Also at University of Belgrade, Faculty of Physics and Vinca Institute of Nuclear Sciences, Belgrade, Serbia
45: Also at Scuola Normale e Sezione dell'INFN, Pisa, Italy
46: Also at National and Kapodistrian University of Athens, Athens, Greece
47: Also at Riga Technical University, Riga, Latvia
48: Also at Institute for Theoretical and Experimental Physics, Moscow, Russia
49: Also at Albert Einstein Center for Fundamental Physics, Bern, Switzerland
50: Also at Istanbul University, Faculty of Science, Istanbul, Turkey
51: Also at Adiyaman University, Adiyaman, Turkey
52: Also at Istanbul Aydin University, Istanbul, Turkey

JHEP04(2018)060

53: Also at Mersin University, Mersin, Turkey
54: Also at Cag University, Mersin, Turkey
55: Also at Piri Reis University, Istanbul, Turkey
56: Also at Gaziosmanpasa University, Tokat, Turkey
57: Also at Izmir Institute of Technology, Izmir, Turkey
58: Also at Necmettin Erbakan University, Konya, Turkey
59: Also at Marmara University, Istanbul, Turkey
60: Also at Kafkas University, Kars, Turkey
61: Also at Istanbul Bilgi University, Istanbul, Turkey
62: Also at Rutherford Appleton Laboratory, Didcot, United Kingdom
63: Also at School of Physics and Astronomy, University of Southampton, Southampton, United Kingdom
64: Also at Instituto de Astrofísica de Canarias, La Laguna, Spain
65: Also at Utah Valley University, Orem, U.S.A.
66: Also at Beykent University, Istanbul, Turkey
67: Also at Bingol University, Bingol, Turkey
68: Also at Erzincan University, Erzincan, Turkey
69: Also at Sinop University, Sinop, Turkey
70: Also at Mimar Sinan University, Istanbul, Istanbul, Turkey
71: Also at Texas A&M University at Qatar, Doha, Qatar
72: Also at Kyungpook National University, Daegu, Korea

JHEP04(2018)060